REPORT DOCUMENTATION PAGE

AFRL-SR-AR-TR-03-

0447

ources, of this fferson

1. AGENCY USE ONLY *(Leave blank)*	2. REPORT DATE	3. REI
	23 OCT 03	FINAL REPORT 1 DEC 99 TO 31 MAY 03

4. TITLE AND SUBTITLE
TAILOR TT-CONJUGATED POLYMERS FOR ENHANCED LUMINESCENCE EFFICIENCY

5. FUNDING NUMBERS
F49620-00-1-0090

2303/CX

61102F

6. AUTHOR(S)
DR. YI PANG

7. PERFORMING ORGANIZATION NAME(S) AND ADDRESS(ES)
CLARK ATLANTA UNIVERSITY
DEPARTMENT OF CHEMISTRY
ATLANTA, GA 30314

8. PERFORMING ORGANIZATION REPORT NUMBER

9. SPONSORING/MONITORING AGENCY NAME(S) AND ADDRESS(ES)
AFOSR/NL
4015 WILSON BLVD., RM 713
ARLINGTON, VA 22203-1954

10. SPONSORING/MONITORING AGENCY REPORT NUMBER

11. SUPPLEMENTARY NOTES

20031104 013

12a. DISTRIBUTION AVAILABILITY STATEMENT
APPROVE FOR PULBIC RELEASE: DISTRBUTION UNLIMITED.

12b. DISTRIBUTION CODE

13. ABSTRACT *(Maximum 200 words)*

During the reporting period, we have systematically examined the role of a meta-phenylene in the tt-conjugated polymers. Resulting form its effective tt-conjugation interruption, controllable insertion of m-phenylene along the polymer backbone is demonstrated to be a useful tool for precise color tuning. Introduction of a bent angle at the m-phenylene unit also improves the molecular packing in the solid state, thereby enhancing the PL quantum efficiency in the solid state. Although original investigation is focusing on the poly(phenylene ethynylene) system, the concept has been successfully extended to poly(phenylene vinylene) system. By synthesis of polymers with defined chemical structures, we have investigated the impact of trace iodine to the luminescent properties of polymers. The results show that the Wittig-Horner reaction is a preferred method to construct the vinylene bond of trans-configuration. It is noted that there are two types of phenyl rings, i.e., m- and p-phenyl rings, present along the PPV chain examined. Selective placement of substituent on the different type of phenyl rings is found to significantly affect the luminescent properties of the polymers. Through collaboration with Professor Karasz's group at UMass, many of the polymers are shown be electroluminescent with EL efficiency reaching as high as `1%. The EL efficiency of this class of materials will be further increased by improving the charge injection within the polymer layer.

14. SUBJECT TERMS			15. NUMBER OF PAGES
			16. PRICE CODE
17. SECURITY CLASSIFICATION OF REPORT	18. SECURITY CLASSIFICATION OF THIS PAGE	19. SECURITY CLASSIFICATION OF ABSTRACT	20. LIMITATION OF ABSTRACT
UNCLAS	UNCLAS	UNCLAS	

Final Technical Report

Project Title: Tailor π-Conjugated Polymers for Enhanced Luminescence Efficiency

Grant No.: F49620-001-1-0090

Period Covered: 01 Dec 1999 – 31 May 2003

PIs: Dr. Yi Pang, Department of Chemistry, Clark Atlanta University, Atlanta, Georgia 30314

Dr. Frank E. Karasz, Department of Polymer Science & Engineering, University of Massachusetts, Amherst, MA 01003

PM: Dr. Charles Y-C Lee, AFOSR/NL
4015 Wilson Blvd, Room 713
Arlington, VA 22203-1954
Phone: (703) 696-7779; Email: charles.lee@afosr.af.mil

Table of Content

Introduction:

The use of fluorescent π-conjugated polymers in emerging technologies, such as LED displays,[1] sensors,[2] and lasers,[3] is rapidly expanding since the first demonstration of an LED device using these polymers in 1990.[4] To be used in commercial applications, the emitting materials must have the qualities required for high performance LEDs such as electrical and thermal stability, processibility, color emission, and luminescence efficiency. To date, there is no organic or polymer material that fulfills all these qualities and such a material still needs to be invented. A variety of polymeric materials have been investigated in search of higher efficiency and better stability.

As an important example in the field, poly(*para*-phenyleneethynylene) (PPE) derivatives[5] have also exhibited many attractive properties. Incorporation of a *meta*-phenylene linkage along the PPE backbone[6] effectively interrupts the π-conjugation, thereby leading to chromophores with defined conjugation length. Introduction of a bent angle along the polymer backbone at the *meta*-phenylene group clearly modifies the chain stiffness, thus leading to the simultaneous improvement[6] in both solubility and luminescence efficiency. Although poly(*m*-phenyleneethynylene)[7] of high molecular weights is reported to be insoluble, the copolymer **2** with both *para*- and *meta*-phenylene units alternately occurring along the chain exhibits good solubility in common organic solvents. The results suggest that alkyl side chains on **2** are still necessary to keep the polymer soluble. Our objectives during the funding period are to further investigate the impact of *m*-phenylene to π-conjugated polymers. Although the initial advantage of an *m*-phenylene in the π-conjugated polymers is observed in PPE, the investigation has been expanded to poly(phenylene vinylene) (PPV) material, which is one of the most promising polymers for LED and laser applications. On the basis of two different types of polymer structures, the report is consisting of two parts. The synthesis and optical properties of *meta*-phenylene-containing PPE are summarized in the part one, and the accomplishments on the PPV materials are in the part two.

Part One. Poly(phenylene ethynylene)s (PPE) with Defined Conjugation Length

1. Synthesis, Chain Rigidity, and Luminescence of Poly[(1,3-phenyleneethynylene)-*alt*-tris(2,5-dialkoxy-1,4-phenyleneethynylene)]s

As a result of the linear bond geometry of acetylene and *para*-phenylene linkages, the polymer backbone of **1** is expected to exhibit a rigid-rod conformation, which is of fundamental and theoretical interest. The Mark-Houwink exponent[8] of **1** has been reported to be $\alpha \approx 1.92$, consisting with its high chain stiffness. A light-scattering study[9] shows that the polymer conformation is nearly rod-like for relative low Mw (< 50 000), but appears to be coil-like in solution for the high molecular weights. Introduction of a bent angle along the polymer backbone at the *meta*-phenylene, however, drastically lowers the Mark-Houwink α exponent to about 0.65 for polymer **2**.[6] A fundamental question remains whether a smaller percentage (i.e., < 50%) of *meta*-phenylene units will be sufficient to improve the solubility and processibility of PPEs. To further evaluate the impact of *meta*-phenylene to the chain rigidity of PPEs, we have synthesized polymer **5**, in which the content of *meta*-phenylene is decreased to 25%. The higher content of *para*-phenylene in **5** will also tune the emission color (red-shift relative to **2**), thereby expanding the application scope of these *meta*-phenylene-based polymers. The regular location of the *meta*-phenyleneethynylene unit along the backbone of **5**, following three consecutive *para*-phenyleneethynylene units, leads to a polymer with a uniformly defined chromophore structure.

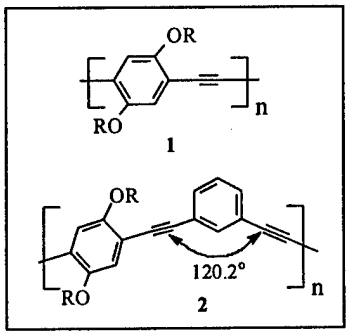

Polymer Synthesis and Characterization. The desired monomer, 1,3-bis[(2,5-dibutoxy-4-ethynylphenyl)ethynyl]benzene derivative **4** was conveniently synthesized by reacting 2,5-dibutoxy-1-trimethylsilylethynyl-4-ethynylbenzene (**3**) with 1,3-diiodobenzene derivatives in the presence of palladium catalyst.[10] Polymerization of **4**

with 2,5-dibutoxy-1,4-diiodobenzene gave polymer **5** as a yellow solid after precipitation from methanol. Infrared spectra of polymer films detected no absorbance at ~3290 cm^{-1} (acetylenic C–H stretch), which is moderately strong in the monomer **4**. Complete polymerization was further confirmed by the ^1H NMR spectra, which showed no acetylenic resonance signals at ~3.35 ppm. The resonance signals at about 4.04 and 4.34 ppm (in a ratio of 6:1) in the ^1H NMR spectrum of **5b** can be attributed to $-OCH_2-$ protons from the alkoxy side chain on the *p*-phenylene and *m*-phenylene, respectively. The presence of only one $Ar-CH_3$ resonance signal at ~2.25 ppm supports the structural regularity along the polymer backbone. Although bearing only short n-butyl side chains, polymer **5** was quite soluble in the common organic solvents such as toluene, chloroform and THF. Uniform thin films could be readily cast from their solutions.

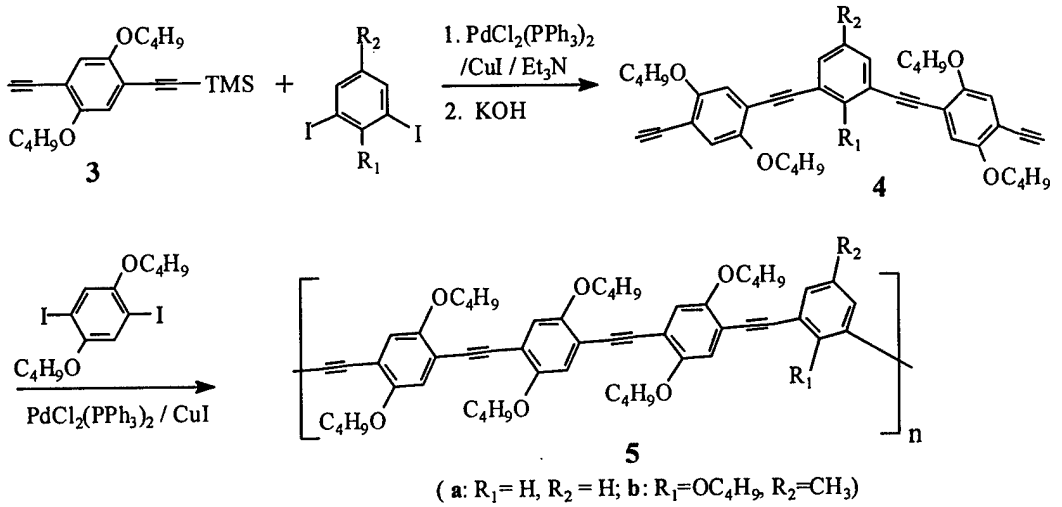

Scheme 1. Polymer Synthesis.

Molecular Weight and Chain Stiffness. The molecular weights of **5**, which are listed in Table 1, were determined in THF by using size exclusion chromatography (SEC) equipped with on-line refractive index (RI), light-scattering (LS), and viscometer detectors (Figure 2). The combination of high molecular weight, low polydispersity (PDI), and monomodal distribution, in addition to the high polymerization yield (~80%), suggested that the polymerization proceeded smoothly as expected. The number-average

degree of polymerization (DP) was estimated to be n ≈ 13 for **5a** and n ≈ 27 for **5b** by using the respective M_n and molecular weight of the respective repeating unit.

By using the on-line viscometer detector, the Mark-Houwink α exponent for polymer **5** was estimated to be ~0.78 in THF solvent at room temperature, which is only slightly higher than α ≈ 0.65 for **2**. The instrument was calibrated by using a broad polystyrene standard, which gave an α value of 0.714 (in agreement with the literature value). The polymer backbone of **5** can be simply viewed as a series of the rigid-rod components **7** joined together via sharing the common *m*-phenylene linkages. Although the rigid-rod length is significantly increased from ~1.65 nm (for **2**) to ~3.01 nm (for **5**), the α value of the polymer is only slightly increased. In summary, the observed Mark-Houwink exponent (α ≈ 0.78) shows that the polymer **5** adopts a random-coil conformation in THF solution.

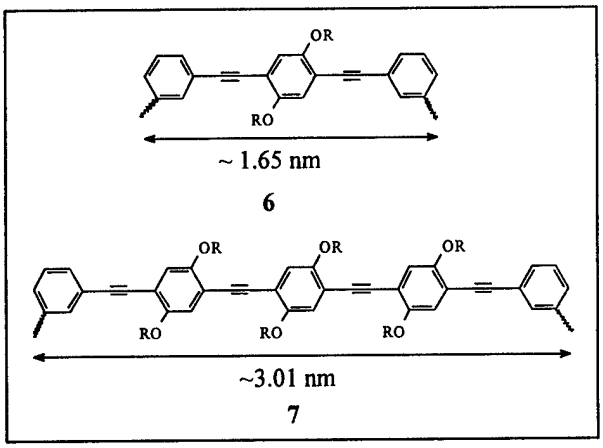

Photoabsorption and Photoluminescence (PL). The UV-vis absorption of **5** in dilute THF (Figure 1) showed a major band at ~ 397 nm (low energy band) and a minor band at about 311 nm (high energy band). In comparison with **2**, the absorption λ_{max} of **5** is noticeably red-shifted from about 376 nm for **2** to ~397 nm for **5**. As a result of the effective π-conjugation interruption at the *m*-phenylene, the effective chromophore for polymers **2** and **5** may be represented by the molecular fragments **6** and **7**, respectively. The bathochromic shift observed from **2** to **5**, therefore, is due to the extended conjugation length in the latter. It is also noted that the high-energy absorption band at ~311 nm remained similar for both **2** and **5**. The relative intensity of the high-energy absorption band, however, decreases with the increased conjugation length. The trend is also consistent with the results observed from **2** and its *para*-phenylene isomer poly[(2,5-dialkoxy-1,4-phenylenevinylene)-*alt*-(1,4-phenylenevinylene)].

Table 1. Molecular Weights and Spectroscopic Data of PPEs.

Polymers	Mw (PDI)	DP	α[a]	UV-vis λ_{max} (nm)[b]		fluorescence λ_{max} (nm)		ϕ_{fl}[c]
				THF	Film	THF	Film	
5a	19 700 (1.8)	13	0.779	311, **397**	325, 414, **446**	**447**, 469(sh)	**487**, 513	0.49
5b	55 100 (2.2)	27	0.776	318, **410**	327, 417, **450**	**449**, 468(sh)	**491**, 520	0.50
2 (R =n-hexyl)	176 900 (1.6)	276	0.650	312, **376**	315, **383**	**405**, 427(sh)	**471**, 494(sh)	0.44

[a]Mark-Houwink exponent were measured in THF at room temperature. [b]The **bold** number indicates the most intense peak. [c]The ϕ_{fl} values were averaged over three independent measurements.

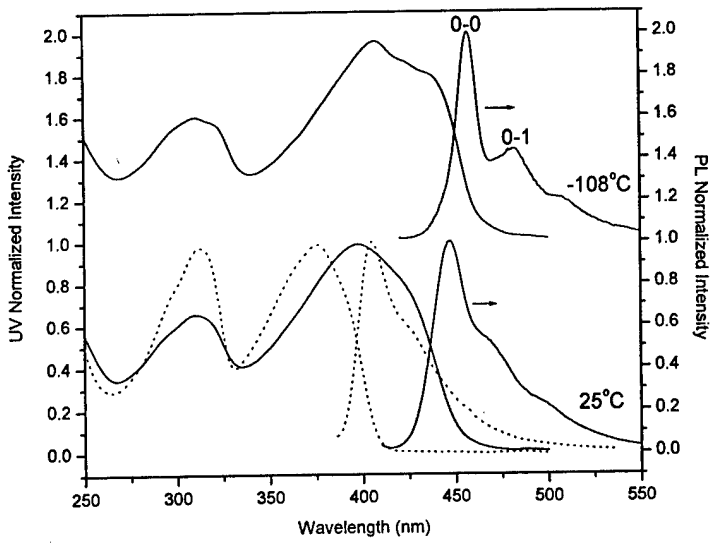

Figure 1. Normalized UV-vis and PL spectra of polymers **5a** (solid line) and **2** (dotted line) in THF. The spectra of **5a** at −108 °C are offset from that at 25 °C for clarity.

The emission profile of **5** is very similar to that of **2**, although the emission λ_{max} of the former is significantly red-shifted from that of the latter (447 nm vs. 405 nm). It is also noticed that the peak width of **5** is essentially the same as that of **2**, with the peak width at half-height of ~34 nm. The narrow emission characteristics of **5** is in agreement with the assumption that the chromophore in the polymer is uniformly defined. The fluorescence quantum efficiency (ϕ_{fl}) of **5** is higher than that of **2**, which could be partially attributed to the higher chain rigidity of the former. The longer conjugation length of **5** (relative to **2**) could be another reason for its high ϕ_{fl} value.

The emission spectrum of **5** at 25 °C exhibited one major peak at about 447 nm and a shoulder at about 469 nm (Figure 6), indicating the existence of vibronic structure. As the temperature was lowered to −108 °C, several emission bands were observed with λ_{max} values at 457, 482, and ~510 nm (corresponding to 21 882, 20 747, and 19 607 cm^{-1}, respectively). The vibrational energy levels in the ground state of **5** (shown from the

emission spectrum) appeared to be about equally spaced with a wavenumber separation of ~1135 cm^{-1}, which is expected from a harmonic oscillator model. The UV-vis absorption spectrum of **5** was also partially resolved at −108 °C, showing an obvious shoulder at ~440 nm (22 727 cm^{-1}). This absorption band ($\lambda_{max} \approx 440$ nm) was separated from the emission band of the highest energy ($\lambda_{max} = 457$ nm) by ~845 cm^{-1}, which is smaller than the required energy gap of 1135 cm^{-1} for a lower energy level in a harmonic oscillator model. The emission bands at 457, 482, and ~510 nm, therefore, are attributed to 0–0, 0–1, and 0–2 transitions, respectively.

To examine the optical properties in the solid state, polymer films of **2** and **5** were prepared by spin-casting their solutions onto quartz substrates. The absorption λ_{max} of films **5a** and **5b** were red-shifted by about 40 nm relative to their respective solution spectra (Table 1), while the film **2** was red-shifted by only ~ 7 nm. The larger bathochromic shift observed from **5** in the absorption spectra is in agreement with the anticipated stronger interaction between chromophores of larger dimension (longer rigid rod) in the solid state. The emission spectra of both films **2** and **5** were significantly red-shifted from their respective solution spectra (~ 66 nm for the former and ~40 nm for the later). The interesting pattern that a significant spectroscopic red-shift from the solution to film states is observed from both the absorption and emission of **5**, but only from the emission of **2**, indicates that a strong polymer chain-chain interaction may start to occur even in the ground state of film **5**. It is also noticed that the absorption and emission spectra of **5** in the solid state become slightly more structured (Figure 2) in comparison with their corresponding solution spectra at room temperature. The high-energy emission peak of **5a** ($\lambda_{max} = 487$ nm) falls at the edge of its absorption profile, suggesting that the emission band at $\lambda_{max} = 487$ nm might originate from a 0–0 transition.

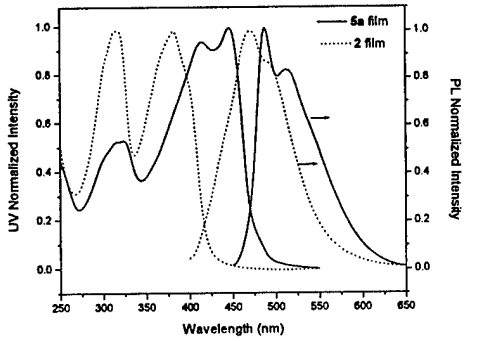

Figure 2. Normalized UV-vis and PL spectra of films **5a** (solid line) and **2** (dotted line).

EL Properties. The high luminescence of the polymer films of **5** indicated potential applications in various devices. A double-layer LED with the ITO/PEDOT/polymer/Ca/Al configuration utilizing polymer **5b** as the emissive layer was fabricated. The device emits green-yellow light as shown in Figure 3. The EL spectra show an obvious voltage dependence: at 12 V and 17 V, the EL peak wavelengths are 577 nm and 547 nm respectively. Thus with an increase of the applied voltage, the EL spectra show a remarkable blue shift of 30 nm. This change in EL is due to Joule heating of the LED at higher current density, which results in a thermochromic effect. The phenomenon can also result from a band-gap distribution in the polymer. At the higher applied voltage, emission from the higher band-gap segments contribute more to the spectrum. Compared with the solid state PL spectrum of **5b**, the EL spectra show obvious red shifts and a substantial spectral broadening. This results from LED interface effects and structural defects in the polymer. The tailing in the long wavelength region can be due to defects in the emissive polymer layer which act as new recombination centers in which excitons radiatively decay yielding an emission different from that given by excitons decaying on the pristine polymer main chain. The LED using **5b** has a turn-on voltage of 8 V and has an external quantum efficiency of 0.013%.

It should be noted that the 0–0 emission band at ~490 nm, which is the most intense photoluminescent emission, becomes the minor peak in the EL spectrum. The 0–1 emission band at ~520 nm, which is well resolved in the PL spectrum, is also observable in the EL spectrum. While emission from the higher vibronic transitions remains a possibility to account for the red-shifted EL emission, the possible presence of a second-optically active species and the formation of an exciplex may also contribute to the spectral mismatch between the PL and EL profiles.

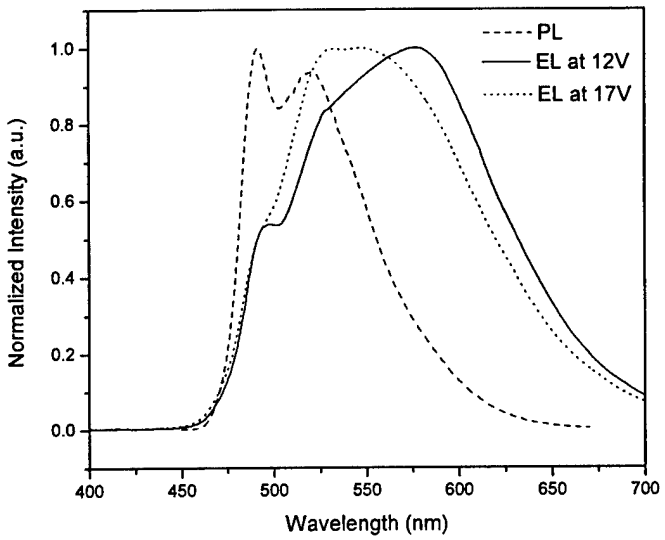

Figure 3. Electroluminescence spectra for device ITO/PEDOT/**5b**/Ca/Al at different voltages. The PL spectrum of film **5b** is also shown for comparison.

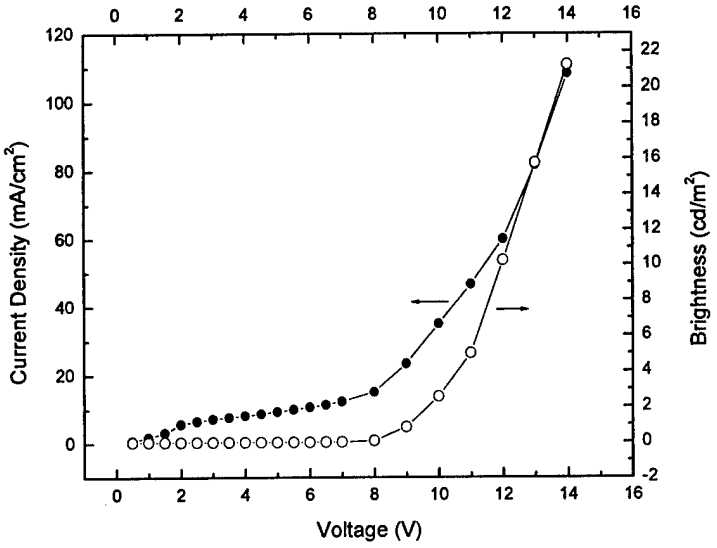

Figure 4. Current density(•)-voltage-brightness(O) relationship for device ITO/PEDOT/**5b**/Ca/Al

Precise Control of Conjugation Length via *m*-Phenylene. One of the great functions of *meta*-phenylene is its interruption on conjugation length. As seen from Figure 5, the electrons of the two substitute groups "A" and "D"on the *para*-phenylene can be delocalized by resonance structure, which allows the conjugation to be extended across the benzene. When the two substituents are placed on the *meta*-phenylene, however, no resonance structures can be drawn to link them. In other words, the two substituents on the *meta*-phenylene are electronically independent, thereby allowing the control of the conjugation length in a predictable fashion. On the basis of the optical absorption and emission properties of polymers **8**,[11] **2**,[6] and **5a**,[10] whose effective chromophores can be described by molecular fragments **9**, **6**, and **7**, respectively, the absorption λ_{max} and emission λ_{max} values are plotted versus the length of *para*-phenylene ethynylene (Figure 6). The fairly good linear correlation shows reliable prediction for the conjugation length of *meta*-phenylene-containing polymers, which is desirable for the emission color control of π-conjugated polymers.

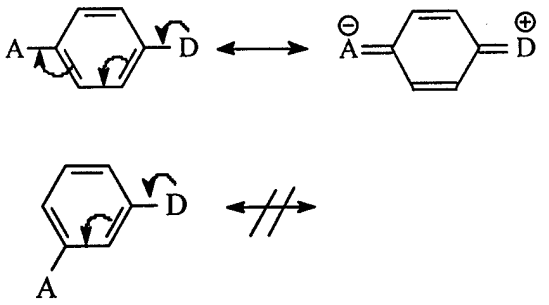

Figure 5. Resonance between the two pare-substituted groups ("A' and "D") allows them to be linked electronically. Resonance between the two meta-substituted groups is forbidden.

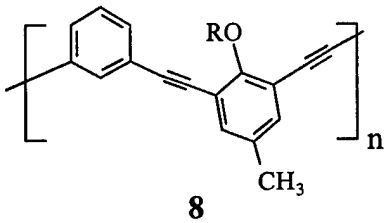

8

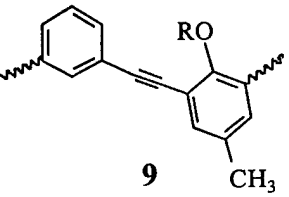

9

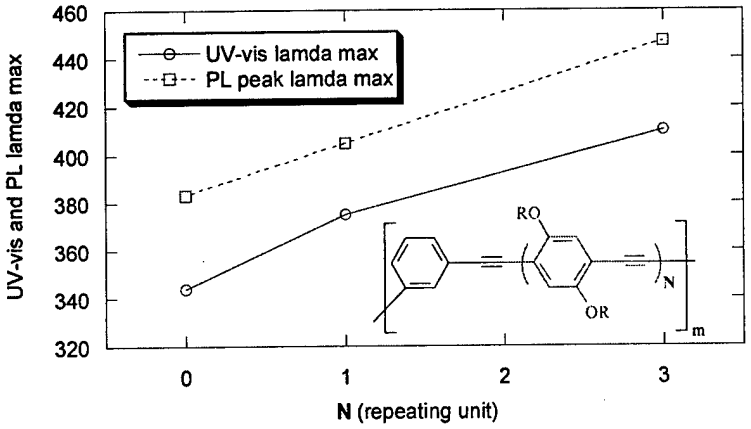

Figure 6. Plot of UV-vis (broken line) and fluorescence (solid line) λ_{max} values in solution versus the block length of *para*-phenylene ethynylene.

2. Poly(phenylene ethynylene)s with Cyano Functional Group

Since the initial observation of electroluminescence from poly(*p*-phenylene ethynylene) **1**,[12,13] a number of studies have been carried out to improve the EL efficiency of PPEs.[14,10,15] As pointed out in the earlier section, the polymer backbone of PPEs has a linear rigid-rod molecular geometry, thus rendering the polymer difficult to process. The rod-like molecular geometry of PPEs is also responsible for their high tendency to form molecular aggregates,[16] which represent an early stage in the transition to a solid state structure and are known to have adverse effects on the luminescence efficiency of π-conjugated molecules.[17,18] Thus, further improvement in luminescence efficiency of PPEs remains a challenge in the field.

Our recent study shows that insertion of an *m*-phenylene into PPE, which leads to the polymer **2**, introduces a bent angle along the polymer chain, thereby simultaneously improving the processibility and luminescence of the materials.[6] In addition, the presence of the *m*-phenylene in **2** reduces the tendency for molecular aggregation,[19] which may contribute positively to the morphological modification in the solid state. To improve the optical properties of **2**, it would be desirable to raise the luminescence

efficiency further. Since a cyano substituent on a phenyl ring often increases the luminescence efficiency of an aromatic molecule,[20] we have investigated polymers of the general structure **10**, which bears the cyano- and alkoxy-groups on the *m*-phenylene ring.

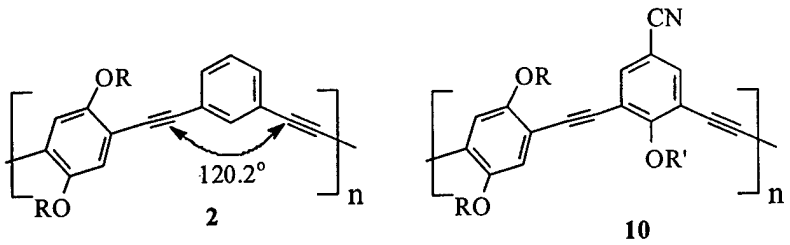

Polymer Synthesis and Characterization. Monomer **12** was synthesized by alkylation of 4-hydroxy-3,5-diiodobenzenecarbonitrile. Coupling[21] between **12** and 2,5-dialkoxy-1,4-diethynylbenzene in the presence of a palladium catalyst generated polymer **13**, which is an example of **10** with a specific alkoxy group on the *p*-phenylene ring. The ^{1}H NMR spectrum (Figure 7) showed two major aromatic protons at 7.0 and 7.7 ppm in about 1:1 ratio, indicating that the reaction proceeded as expected to incorporate both *m*- and *p*-phenylene units along the polymer chain. This was further confirmed by the observation of two different $-OCH_2-$ groups at 4.5 (on *m*-phenylene) and at 4.0 ppm (on *p*-phenylene) in an approximately 1:2 ratio. The two minor aromatic proton signals between 7.3 and 7.5 ppm are attributed, at least in part, to the phenyl groups at the chain ends. Polymer **13** exhibited good solubility in common organic solvents such as THF, chloroform, and toluene. The size exclusion chromatography (SEC) analysis of **13** (Figure 8) showed that the polymer had a monomodal distribution with normal polydispersity (PDI≈1.9-2.4), which is in agreement with the proposed linear polymer chain structure. Uniform thin films could be conveniently cast from the polymer solutions.

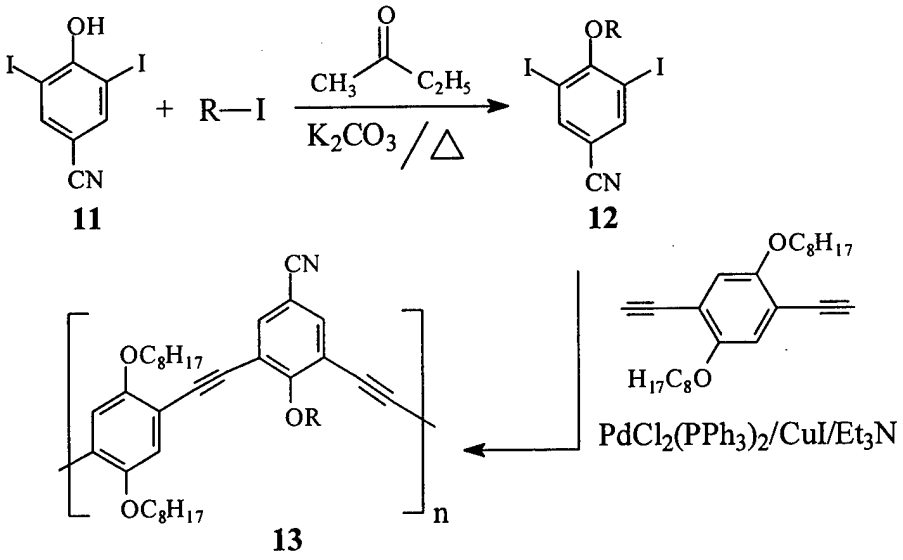

a: R = n-C_4H_9; b: R = n-C_6H_{13}

Scheme 2. Synthesis of cyano-containing PPEs.

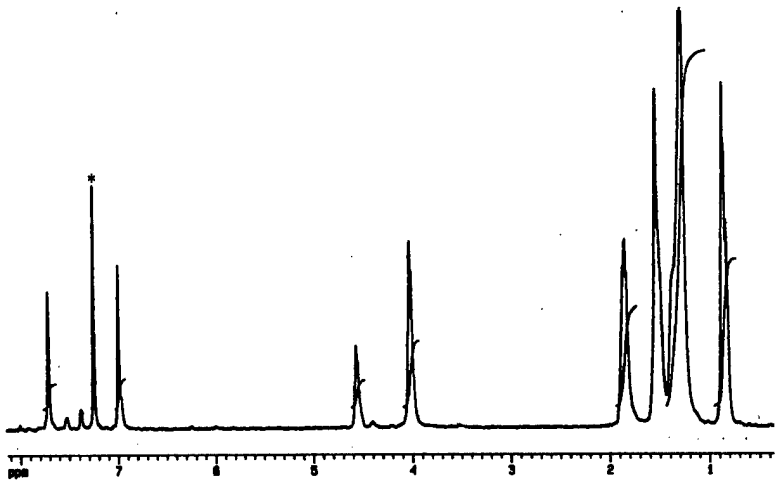

Figure 7. ^{1}H NMR spectrum of **13b** in $CDCl_3$. The starred signals at 7.25 ppm is attributed to $CHCl_3$ solvent.

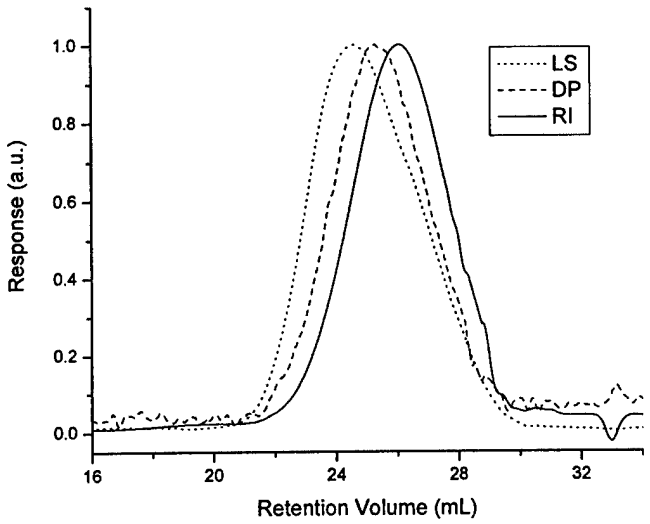

Figure 8. Size Exclusion Chromatography (SEC) chromatogram of **13b** with on-line refractive index (RI), viscosity (DP), and light-scattering (LS) detectors.

Absorption and Photoluminescence (PL). UV-vis absorption spectrum of CN-PPE in THF exhibited two maxima with λ_{max} ≈315 and 395 nm (Table 2 and Figure 9). The absorption λ_{max} of **13** was red-shifted by about 20 nm from that of **2** (λ_{max} ≈ 375 nm, Table 2) as a result of additional cyano and alkoxy substituents at the *m*-phenylene of the former. Resulting from the effective π-conjugation interruption at adjacent *m*-phenylene units, the chromophores in polymers **2** and **13** can be represented by the molecular fragments **14** and **15**, respectively. Therefore, each pair of alkoxy and cyano substitution on the chromophore contributed about 10 nm increment in the absorption maximum. The observed small substitution effect[22,23] in **13** could be attributed to the

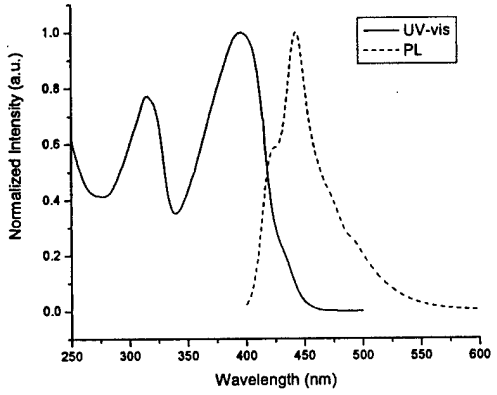

Figure 9. UV-vis (solid line) and PL (broken line) spectra of CN-PPE (OC6) in THF.

fact that the cyano group is *meta*-linked relative to the C≡C triple bonds, which prevents it from achieving an effective interaction with the primary π–π^* absorption band along the polymer backbone.

Table 2. Spectroscopic comparison between PPEs **2** and **13**.

PPE polymers	M_w (PDI)	Absorption λ_{max} (nm)[a]	Fluorescence λ_{max} (nm)[a]	Excitation λ_{max} (nm)[a]	ϕ_{fl}[b]
13a	29,450 (2.3)	315, 394	422 (sh), 444	394	0.63
13b	21,200 (1.9)	315, 399	423 (sh), 443	392	0.60
2 (R= hexyl)	77,900 (2.4)	310, 375	405, 425 (sh)	377	0.44

[a]UV-vis absorption and fluorescence data were obtained from their respective THF solutions. [b]Fluorescence quantum efficiencies were measured in relative to quinine sulfate standard[24] while polymer solutions were excited at their absorption maxima.

Fluorescence of **13** showed a shoulder at about 423 nm, and a maximum at 443 nm, attributed to the 0–0 and 0–1 vibrational transitions. This assignment was further confirmed by acquiring the PL spectrum of **13** at different temperatures (Figure 10). As the temperature was lowered, the emission shoulder at ~423 nm (0–0 transition) was resolved into a pronounced peak. The relative emission intensity of the 0–0 transition showed a temperature dependence such that at 25 °C, the most intense emission was from the 0–1 transition, whose intensity gradually decreased as the temperature was lowered. At –198 °C, the relative weak emission band at ~423 nm (0–0 transition) became the more intense. It appeared that the relative emission intensities among the different transitions were dependent, at least in part, on the chromophore environment rigidity, which is a function of temperature.[25] The fluorescence quantum efficiency of **13** in THF solution was estimated to be about $\phi_{fl} \approx 0.6$, significantly higher than that of the parent polymer **2** ($\phi_{fl} \approx 0.44$). The presence of alkoxy and cyano substituents clearly played an important role in the luminescence enhancement, although it was not clear whether their *co*-existance was a significant factor.

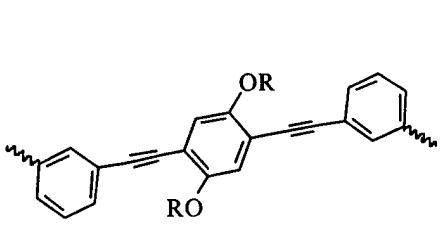

14

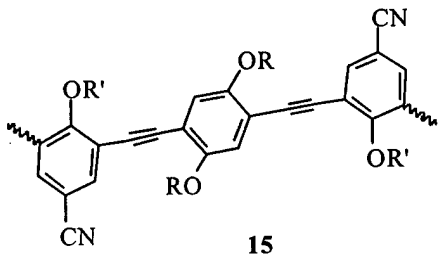

15

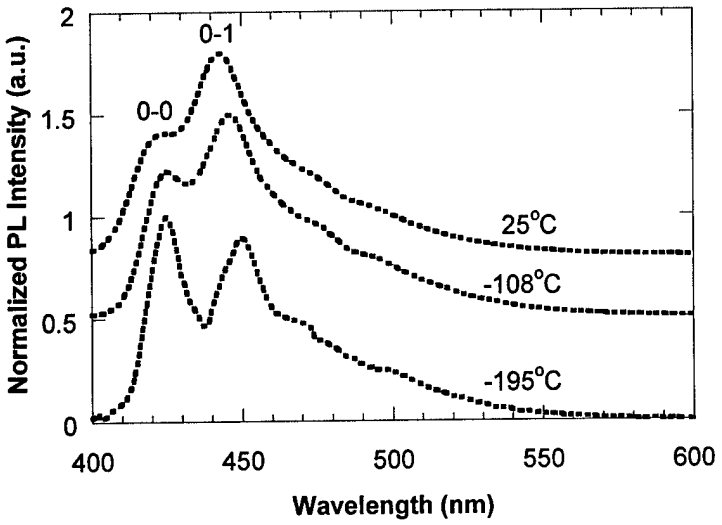

Figure 10. Photoluminescence of **13b** in THF at 25, −108, and −195 °C. The spectra at different temperatures are offset for clarity.

Optical Properties of the Polymer Films. The solid-state spectra were acquired from polymer films spin-cast on quartz plates. The UV-vis absorption of film **13** exhibited nearly the same profile as its solution spectra, showing two absorption bands with $\lambda_{max} \approx 328$ and 428 nm (Figure 11). The similarity between the solution and film spectra supports the assumption that the chromophore in the polymer is well-defined. The absorption λ_{max} of film **13** was red-shifted from its solution λ_{max} by about 29 nm, which was larger than the bathochromic shift of ~10 nm observed in **2**. The larger

bathochromic shift observed from the solution to film spectra of **13** is consistent with its polymer chain structure, as the polar cyano substituent on the polymer chain increases the chromophore-chromophore interaction in the solid state. It should also be noted that the absorption of film **2** exhibited two bands of about equal intensity. The relative intensity of the high energy absorption band in the film **13** (at about 325 nm) significantly decreased as a result of additional cyano and alkoxy substituents on the *m*-phenylene.

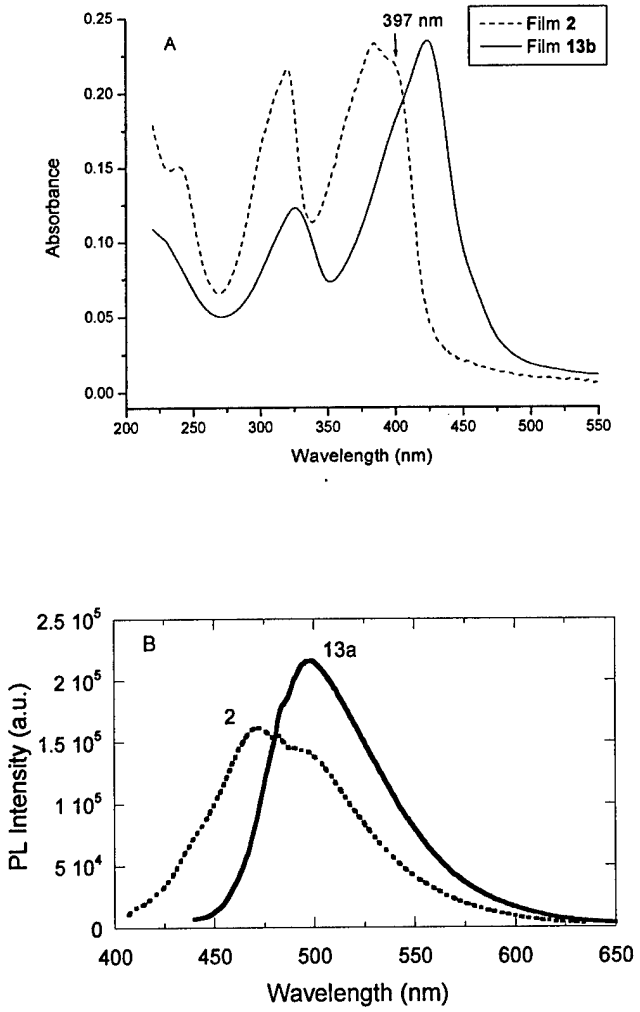

Figure 11. UV-vis (A, top) and fluorescence (B, bottom) spectra of films **2** and **13b** on quartz plates.

EL properties

To test the EL properties, polymer **13b** was used to fabricate LED devices. Green-yellow emission was observed from a double-layer device with ITO/PPV/**13b**/Ca configuration, where PPV was used as a hole-transport layer. The EL spectrum (Figure 12) showed two peaks at 521 and 552nm, and one minor shoulder at 602 nm. The major EL emission band of **13b** at 552 nm was notably red-shifted compared to its film PL emission band, and was attributed to the emission of **13b**. The minor band at 521 nm could be originated from the EL emission from the PPV layer, since its single layer device (ITO/PPV/Ca) gave green emission at 500 and 529 nm (Figure 12, curve b). Observation of both minor bands at 521 and 602 nm, however, suggested that they belonged to the vibronic structures of **13b**. It should be noted that the EL emission from the PPV layer in the double layer device would be very low as the EL emission of ITO/PEDOT/**13b**/Ca also started at 450 nm (Figure 13). The maximum brightness and external quantum efficiency for device ITO/PPV/**13b**/Ca were found to be 20 cd/m^2 and 3.7×10^{-4}% respectively.

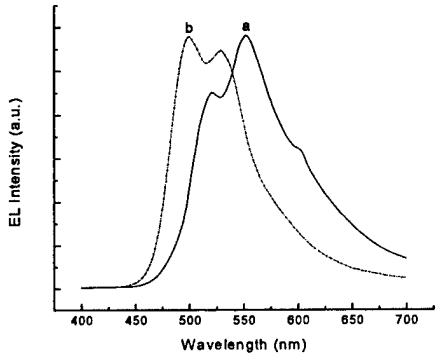

Figure 12. EL comparison between devices ITO/PPV/**13b**/Ca (a) and ITO/PPV/Ca (b).

The EL spectrum for the double-layer device ITO/PEDOT/**13**/a (Figure 13) was significantly broader than that for ITO/PPV/**13b**/Ca, showing the effect of the hole-transport layer. This was consistent with the observation that the emission of **13** was quite sensitive to its environment (Figure 10). The emission peak of the device ITO/PEDOT/**13b**/Ca was also found to be dependent on the voltage applied. A yellow emission with the EL peak wavelength at 551 nm was observed at 22 V, which shifted to 594 nm at 31 V.

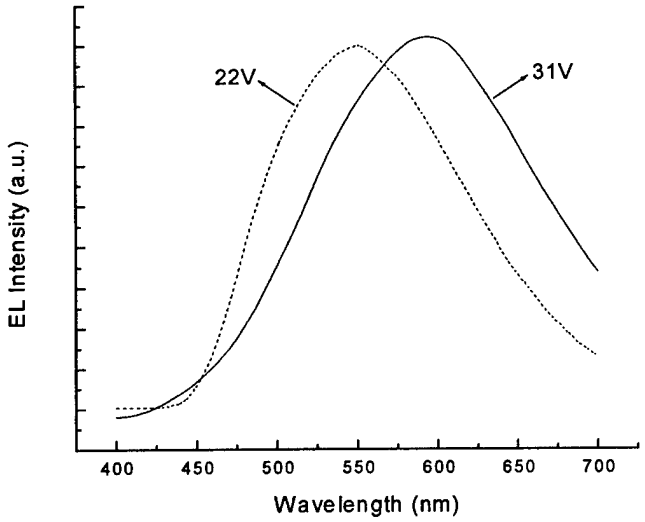

Figure 13. EL spectra for the double-layer device ITO/PEDOT/**6b**/Ca under different applied voltage.

Part Two: Inclusion of *meta*-phenylene unit in poly(phenylene vinylene) (PPV)

1. Impact of Side Chain Length to Luminescence of Poly[(*m*-phenylene vinylene)-*alt*-(*p*-phenylene vinylene)]

On the basis of our recent study, introduction of *meta*-phenylene unit into the linear rod-like chain of PPE **1** simultaneously improves the solubility and enhances the photoluminescence efficiency of the polymers. Reasoning that the simultaneous enhancement in PL and solubility could also be observed in PPV, we have synthesized poly[(*m*-phenylene vinylene)-*alt*-(*p*-phenylene vinylene)] derivatives **17** with various substituents. The polymers are yellow solids with the molecular weights ranging from 19,000 to 25,000. The olefins in the polymers are present in both *cis*- and *trans*-configuration. On the basis of acquired ^{1}H NMR spectra, the ratio of the *cis*-/*trans*-olefin bond in the polymer is estimated to be about 6:4. Polymers **17** are soluble in common organic solvents (toluene, THF, chloroform), although they only bear short alkyl side

chains. This finding confirms that the presence of *meta*-phenylene linkage plays an important role to improve the solubility.

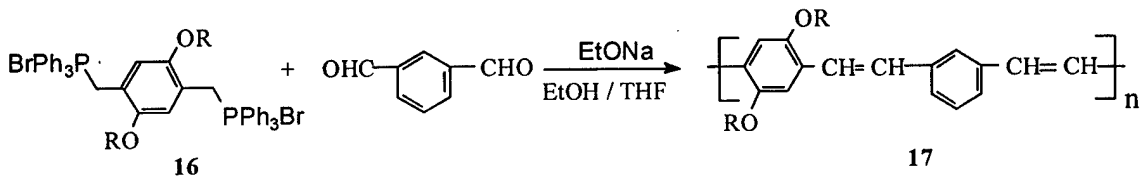

a: R= n-C_6H_{13}; b: R= n-C_4H_9; c: R= C_2H_5

An essential element in our study is to examine the influence of *meta*-phenylene linkage in the polymer to the luminescent properties of the materials. Polymers **17** are highly luminescent in solution, with solution PL efficiency estimated to be $\phi_{fl} \approx 0.80$-0.82 (emission centered at about 470 nm). The polymer films, spin-cast from their solutions, are also found to be highly luminescent with emission peaked at about 504 nm (green color). Direct comparison shows that the film **17a** is about 4.5 times as high as the standard PPV film. The high PL efficiency of film **17** is estimated to be about 80% by direct comparison with 9,10-diphenylanthracene dispersed in a PMMA film. Polymers **17a** and **17b** have been used to fabricate LED devices. Figure 14 shows the EL spectra of **17a** and **17b** from double layer devices. It appears that the length of the side chain does not affect the EL spectra. The device from **17b**, however, appears to be more stable than the corresponding device from **17a**, indicating that the side chain do have some impact on the device stability.

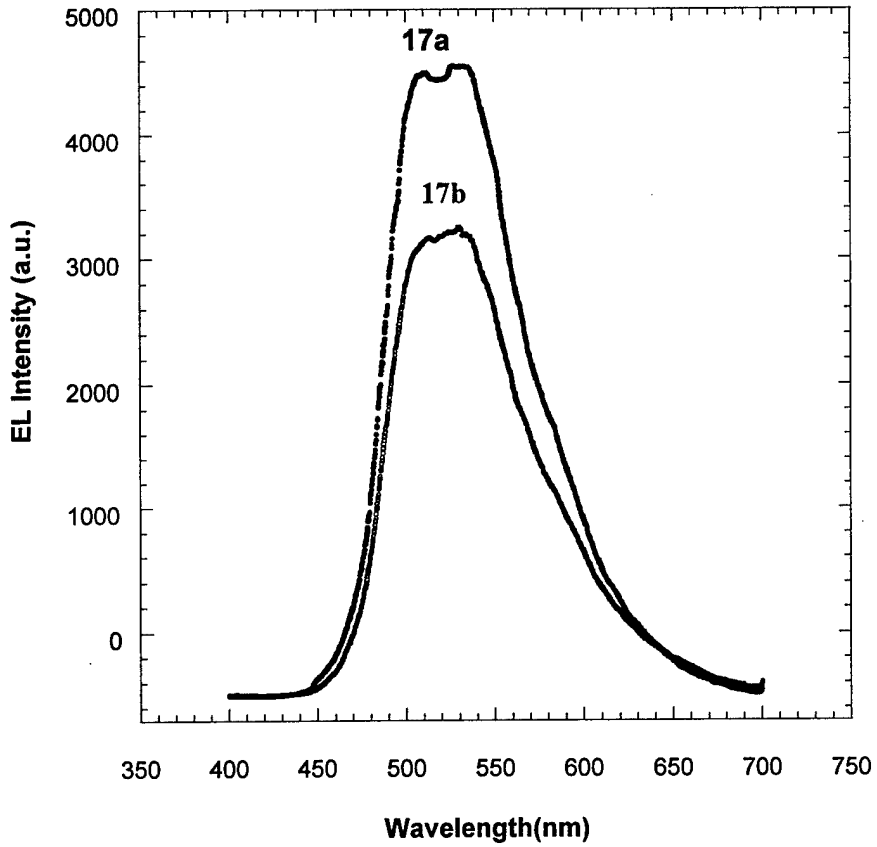

Figure 14. Electroluminescence spectra of double layer devices (ITO/PPV/m-PPV **17**/Ca) under driving pulse voltage (10V).

2. Impact of Trace Iodine to the Optical Properties of PPV

Recent studies[26] have shown that poly[(*m*-phenylenevinylene)-*alt*-(*p*-phenylenevinylene)] derivatives **17** (PmPVpPV) are green-emitting with high photoluminescence (PL) efficiency. The polymers are generally synthesized via using the Wittig condensation reaction (Scheme 3). The majority[6a] of the vinylene linkages in the polymers **17** are in the *cis*-configuration. To reduce the chain defects in the polymer, which may adversely affect the optical properties, it is desirable that the vinylene bonds in **17** are in the thermodynamically more stable *trans*-configuration. Although polymer **18** with *trans*-vinylene linkages can be obtained by refluxing the toluene solution of **17** in the presence of a catalytic amount of iodine, the polymer thus obtained may be contaminated by iodine, which is known to decrease the PL quantum yield[27] via the so-called "heavy-atom" effect. In the iodine-catalyzed isomerization, the reaction may proceed via a thermally induced iodine radical process as proposed in the conjugated olefin system.[28] Although only a catalytic amount of iodine (~0.2-0.3% by weight) is used in the reaction, some iodine atom may be chemically bonded to the product to generate some structural defects along the polymer backbone, which may adversely affect the optical properties of the polymers.

The iodine-free PmPVpPV with a high content[29] of *trans*-vinylene linkages (**20b**) has been synthesized via the Wittig-Horner reaction. The solution PL efficiency of **20b** ($\phi_{fl} \approx 0.64$ in THF) is measured to be the same as that of **18b**, while the PL emission λ_{max} of the former is slightly red-shifted ($\Delta\lambda_{max}$ = 1-2 nm). To further evaluate the impact of the iodine treatment to the optical properties of PmPVpPV samples, especially in the film state, we have made a comprehensive comparison between polymers **18** and **20**, which have similar content of *trans*-vinylene linkage. Since the iodine-catalyzed isomerization remains to be a common method used in synthesizing poly(phenylenevinylene) (PPV) materials,[30,31,] understanding the overall impact of the iodine treatment to the π-conjugated polymers, therefore, is desirable for the future development of luminescent polymers.

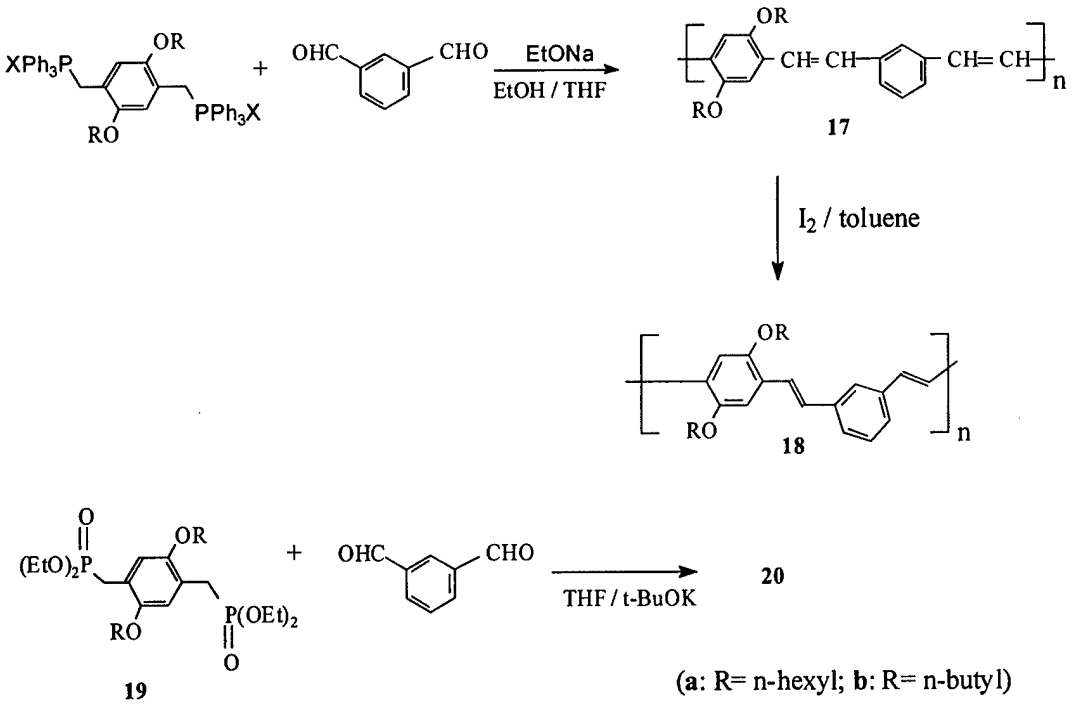

Scheme 3. Synthesis of PPVs via the Wittig or Wittig-Horner reaction.

The iodine-catalyzed isomerization of *cis*-1,2-diarylethene (**21**) might proceed similarly as proposed for the isomerization of conjugated dienes.[32] As shown in the Scheme 4, addition of an iodine radical to **21**, followed by rotation of the carbon-carbon single bond, produced the radical **22**. Regeneration of the iodine radical from **22** would lead to the desired *trans*-1,2-diarylethene (**23**). Hydrogen abstraction from **22** or recombination of **22** with an iodine radical produced the respective iodine-contaminated structures **24** or **25**. Elemental analysis of **18a** showed that the sample contained ~0.26%

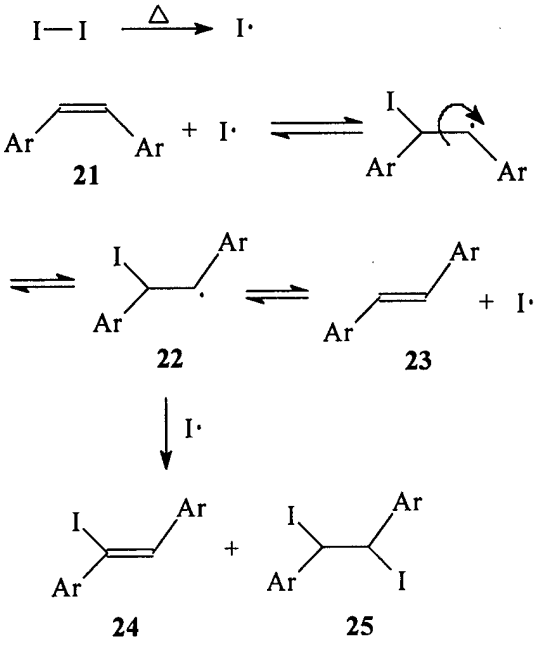

Scheme 4. Mechanism of iodine-catalyzed isomerizartion.

iodine elements, indicating that about 1 per 241 phenylenevinylene units[33] might contain an iodine atom introduced during the isomerization process. The average number of phenylenevinylene units for polymer **18a** is estimated to be only 71, by using the number-average molecular weight. This result suggests that only a small fraction (less than 0.3%) of polymer chains is contaminated by iodine. Both infrared and NMR (^{1}H and ^{13}C) spectra detected no difference between polymers **18** and **20**, supporting the assumption that the iodine-contamination in the former would be very low.

Photoabsorption and Photoluminescence of Solutions. Figure 15 shows the UV-vis spectra of **18a** and **20a** in THF solution at room temperature, exhibiting two absorption bands (λ_{max} = 328 and ~406 nm). The λ_{max} value of the low energy absorption band was measured to be 406 nm and 410 nm for polymers **18a** and **20a**, respectively. As the temperature was lowered from 25°C to −108°C (still in solution state), both spectra were red-shifted similarly, indicating the adoption of a more planar conformation at the low temperature. In addition, the low energy absorption band was resolved into two bands at −108°C (λ_{max} = 415 and 437 nm for **18a**; and λ_{max} = 420 and 438 nm for **20a**), due to the reduced rotation and increased solvent viscosity at the low temperature.

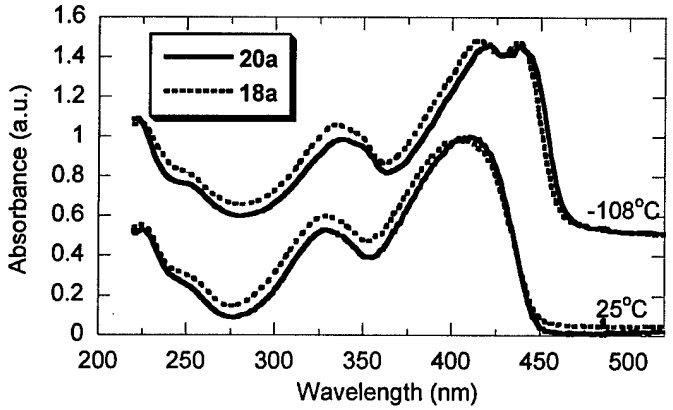

Figure 15. UV-vis spectra of **20a** (solid line) and **18a** (broken line) in THF at 25°C and −108°C. The spectra at different temperature are offset for clarity.

Table 3. Comparison of Spectroscopic Data for PmPVpPV **18** and **20**.

Polymer	Content of *trans*-CH=CH	UV-vis λ_{max} (nm)[a]	Fluorescence λ_{max} (nm)[a]	Film UV-vis λ_{max} (nm)	Film PL λ_{max} (nm)	ϕ_{fl}[b]	*Mw* (PDI)[c]
18a	91	328, 402	444, 469	335, 411	506, 532	0.65	25 000 (1.4)
20a	88	328, 404	445, 471	336, 412	503, 531	0.64	11 590 (2.1)
18b	95	328, 407	447, 475	336, 422	507	0.60	20 200 (1.4)
20b	96	328, 410	447, 475	337, 422	530	0.63	45 000 (2.0)

[a]The optical data is acquired from the THF solution at room temperature. [b]The fluorescence quantum efficiency values are estimated in THF solution by using the conditions reported previously. [c]M_w and PDI of the polymers are determined by using gel permeation chromatography equipped with on-line refractive index, light-scattering, and viscometer detectors.

Fluorescence spectra of **20a** and **18a** at room temperature (Figure 16) revealed very similar emission profile with emission λ_{max} at 447 and 475 nm. The solution fluorescence quantum efficiency ϕ_{fl} (Table 3) for polymers **18** and **20** were comparable. Although both polymers gave more intense emission at 447 nm, their relative emission intensities at 475 nm were different. The possible iodine contamination in **18**, therefore, appeared to have only small effect on the luminescent property of the molecule, which is in agreement with the fact that the concentration of the iodine-contaminated repeating unit is very low.

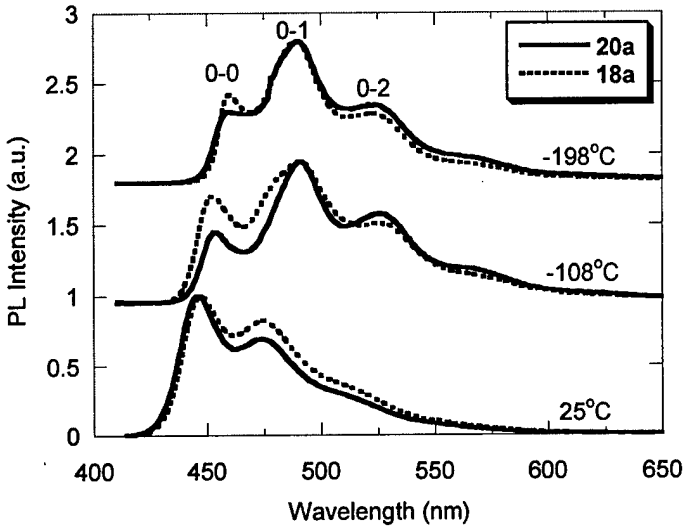

Figure 16. Normalized solution PL spectra of **20a** (solid line) and **18a** (broken line) at 25°C and −108°C in THF, and at −198°C in a solvent mixture (diethyl ether, ethanol, and 2-methylbutane in a ration of 1:1:1). The spectra at different temperature are offset for clarity.

As the temperature was lowered to −108°C, the spectra were also noticeably red-shifted with emission peaks at 454, 491, and 526 nm (corresponding to the wavenumber of 22026 cm^{-1}, 20367 cm^{-1}, and 19011 cm^{-1}, respectively). The emission peaks appeared to be about equally spaced with a wavelength separation of ~35 nm (or a wavenumber separation of ~1659 cm^{-1}), which is larger than the difference between the high-energy

emission band (at 454 nm) and the low-energy absorption band (at ~437 nm). Based on the theoretical model[34] of an Anharmonic Oscillator, the emission peaks of 454, 491, and 526 nm in the spectrum of –108°C were assigned to the 0–0, 0–1, and 0–2 transitions, respectively. Interestingly, the 0–1 band became the most intense emission at –108°C. When the temperature was lowered to –198°C (sample was completely frozen), the relative intensity of 0–1 band was further slightly increased at the expense of 0–0 band. This change in relative emission intensity was apparently related to the molecular conformation change at the low temperature, which was observed from the bathochromic shifts in both absorption and fluorescence spectra.

Thin Film Optical Properties. Figure 17 showed the absorption spectra of films cast on the quartz surface. The absorption profile of **18a** overlapped very well with that of **20a** at room temperature. As the films were immersed in liquid nitrogen (at –198°C), however, the spectrum of **20a** was noticeably red-shifted (~8 nm) from that of **18a**. As previously shown from their solution absorption spectra (Figure 15), the chromophores in both **20a** and **18a** had the similar tendency to adopt a more planar molecular conformation at the low temperature. The tendency for the chromophores in the polymers to achieve a more planar conformation was greatly reduced in the film state, as the motion of the polymer chains was restricted. The observed bathochromic shift of the film **20a** from the film **18a** at the low temperature suggested that the chromophore in the former was packed in a slightly different environment than that in the latter. The presence of the small amount of the structural defects present in **18a** could interfere with the molecular packing in the film state, thereby resulting in a difference between the packing environments for the films **18a** and **20a**.

At –198°C, the broad low-energy absorption band of **20a** appeared to be resolved into two peaks (λ_{max} at 425 and 446 nm), attributing to the further reduced vibration and rotation at the low temperature. The difference ($\Delta\lambda_{max}$ =21 nm) between the two newly resolved peaks in the film **20a** at the low temperature matched very well with that ($\Delta\lambda_{max}$ =18 nm) observed from its solution at –108°C, indicating that the resolved absorption

bands in the film were intrinsic molecular property of the chromophore in the polymer. In comparison with the film **20a**, the absorption band of **18a** was less resolved at –198°C, which seemed to be in agreement with the assumption that the chromophore in the latter had a less planar conformation.

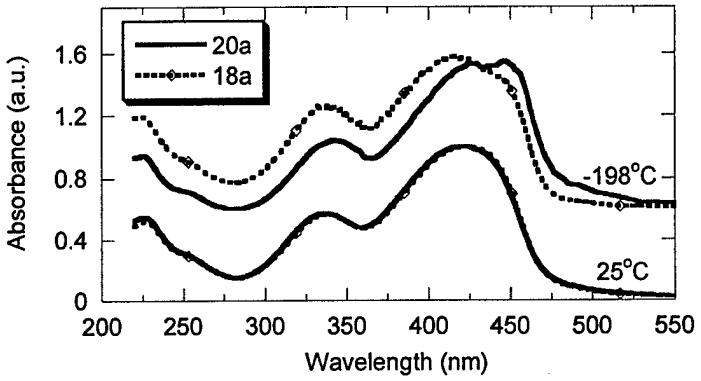

Figure 17. UV-vis spectra of films **20a** (solid line) and **18a** (broken line) on quartz at 25°C and –198°C. The spectra at different temperature are offset for clarity.

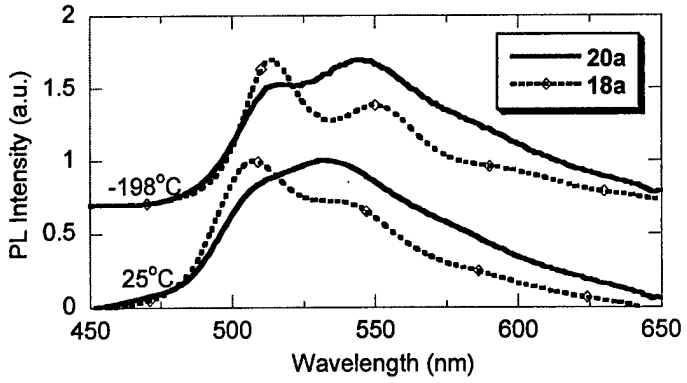

Figure 18. PL spectra of films **20a** (solid line) and **18a** (broken line) on quartz at 25°C and –198°C. The spectra at different temperature are offset for clarity.

Although the absorption spectra of films **18a** and **20a** exhibited nearly the same profile at room temperature, their PL spectra showed noticeable difference (Figure 18). At –198°C, the broad emission peak of film **20a** was partially resolved into two bands with λ_{max} at 516 and 544 nm, which matched very closely with the emission peaks of 516 and 549 nm from the film **18a**. The observed similarity in the vibronic structure of films **18a** and **20a** confirmed the presence of the same emission chromophore in both polymers. Polymers **18a** and **20a** exhibited quite different emission intensity ratio at peaks 516 and 544 nm, indicating the potential influence of different sample preparation on the luminescent property. In addition, the PL spectra of the polymer at –198°C were slightly red-shifted (about 7-14 nm) from that at room temperature. This PL spectral red-shift is much smaller than that observed from MEH-PPV films (~32 nm)[35] when the temperature was changed in a similar range (from 12°C to –192°C), partially attributed to the defined conjugation length present in both **18** and **20**.

The corresponding wavenumber for the emission peaks at 516 and 544 nm are 19380 cm^{-1} and 18382 cm^{-1}. The wavenumber separation between the adjacent vibronic energy levels in the films, therefore, was estimated to be 998 cm^{-1}. The wavenumber separation between the absorption band of the lowest energy at 466 nm (21459 cm^{-1}, Figure 17) and the emission band of the highest energy at 516 nm (Figure 18) was estimated to be 2079 cm^{-1}, which was slightly more than twice as large as the adjacent viberational energy gap of ~998 cm^{-1} in the ground state (observed from the emission spectrum). The large separation between the absorption band at 466 nm and the emission band at 516 nm suggested that the emission peaks at 516 nm and 544 nm from the films could originate from the 0–1 and 0–2 transitions, respectively. The assignment appeared to be in agreement with the observation from the solution PL spectra, where the emission from the 0–1 and 0–2 transition increased greatly at the expense of the 0–0 emission when the molecule was frozen into a rigid environment (Figure 16).

In order to examine the PL quantum efficiency, thin films of **20a** and **18a** were prepared on quartz plates. To minimize the effect of film thickness, the films were spin-cast from their solutions so that their absorbance values at absorption λ_{max} were between 0.09-0.1. At room temperature, film **20a** exhibited constantly higher emission intensity than that of **18a**. The observed larger impact from the trace iodine element in the polymer films, in comparison with their solution PL efficiencies, could be rationalized by considering the interaction between the trace iodine element and polymer chain. In the dilute solution, interaction between iodine and polymer chain is predominantly limited to intramolecular interaction. In the films, however, the intimate packing of polymer chains permits the trace iodine element to interact both intra- and inter-molecularly with the neighboring polymer chains, thereby allowing each iodine atom to exerting influence on more than one molecules.

EL Properties. LED devices were fabricated under the identical experimental conditions to compare the EL properties. The double layer device ITO/PEDOT/**18a** or **20a** /Ca gave green emission, although the emission peaks of **18a** (at 513 and 539 nm) was slightly red-shifted from that of **20a** (513 and 523 nm). The EL spectra (Figure 19) of **18a** and **20a** conformed very well with their respective film PL spectra, indicating that both PL and EL originated from the same radiative decay process of the singlet exciton.[16] Turn-on voltage for the device of **20a** (~3.5 V) was noticeably lower than that for **18a** (~5 V). In addition, the external quantum efficiency for the device of **20a** (0.16%) was remarkably higher than that for **18a** (0.036%). The drastic improvement in the device efficiency is apparently due to the balanced electron/hole injection achieved in the polymer layer **20a** (Figure 20). The lower EL efficiency of **18a** is clearly associated with the presence of trace iodine contaminant, which lowers its PL efficiency in the film state.

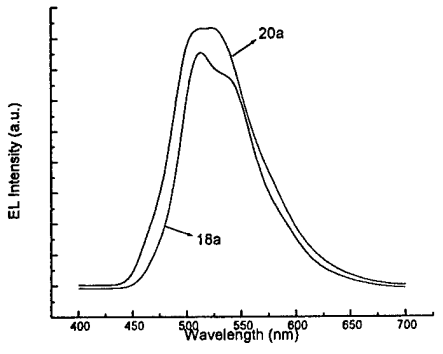

Figure 19. EL spectra of **18a** and **20a** with the device configuration ITO/PEDOT/polymer/Ca.

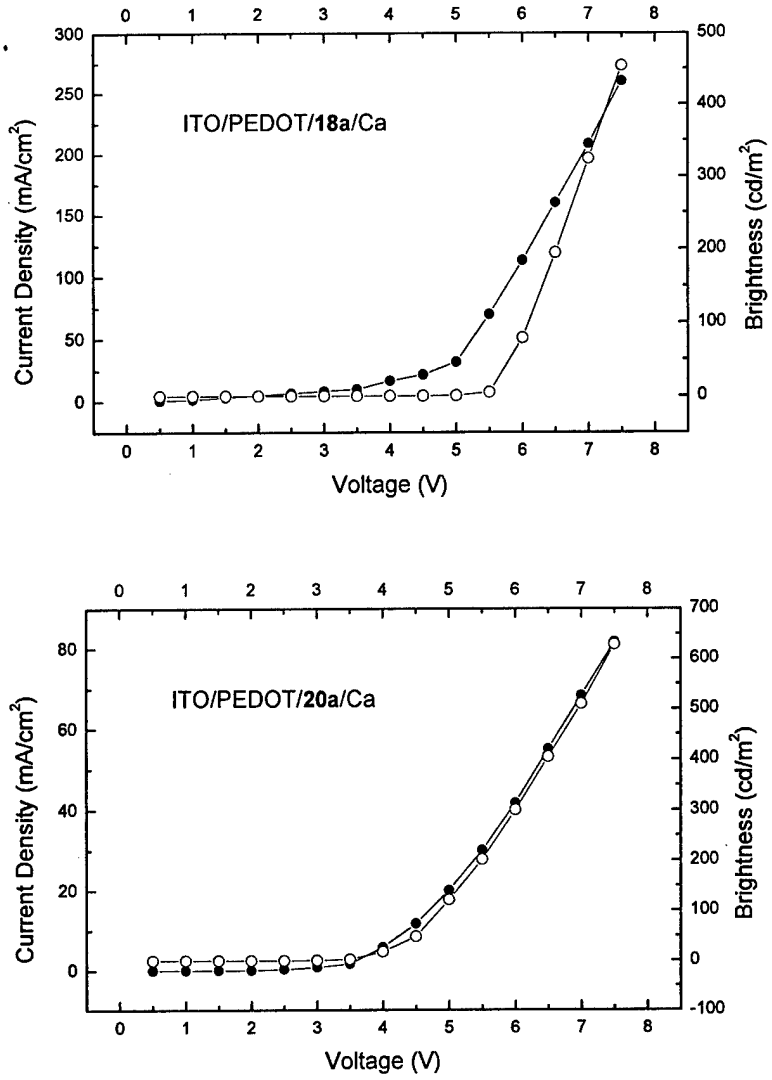

Figure 20. Current density-voltage-brightness relationship for the device ITO/PEDOT/**polymer**/Ca.

In summary, a systematic study has been carried out to investigate the influence of the iodine-catalyzed isomerization on the optical properties of PmPVpPV. Although little effect is observed in solution, the potential contamination from the iodine-catalyzed

isomerization exhibits noticeable influence on the optical properties of the polymer films, especially at the low temperature. With the aid of the low temperature spectroscopic study, the majority of emission from the films are likely originating from the 0–1 and 0–2 transitions. Electroluminescent characteristics shows that the iodine contamination may cause imbalanced electron-hole injection, thereby lowering the device efficiency. The iodine-free polymer permits a balanced injection of electron-hole, thus greatly improving the EL efficiency to 0.16% in a device configuration of ITO/PEDOT/polymer/Ca.

3. Impact of Substitution Pattern to Luminescence.

As discussed in previous sections, poly[(*m*-phenylenevinylene)-*alt*-(*p*-phenylenevinylene)] (PmPVpPV) derivatives (**20**)[26,36-39] are green-emitting with high photoluminescence (PL) efficiency. It is noted that the phenylene units in PmPVpPV are linked alternately at *meta*- and *para*-positions. While the alkoxy substituents in **20** are placed only on *p*-phenylene, we have investigated the optical properties of PmPVpPV **26** which bears substituents solely on *m*-phenylene.[40] The results show that substitution on the different type of phenylene rings can affect the optical properties (emission wavelength and efficiency) of the respective materials in a different way.

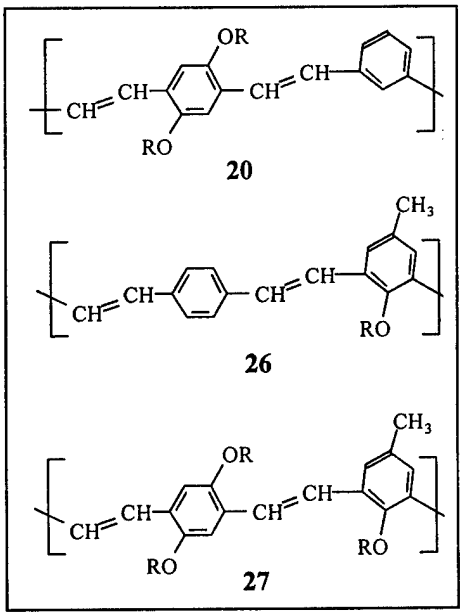

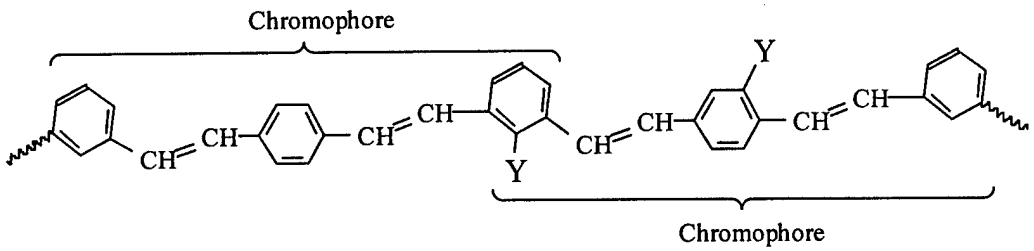

28

The molecular fragment **28** represents a section of PmPVpPV backbone. Benefiting from the effective π-conjugation interruption at *m*-phenylene linkage, the chromophore in PmPVpPV can be described as *p*-phenylenedivinylene sandwiched between the two adjacent *m*-phenylene units. Depending on the location of substituent "Y" on the *p*-phenylene or *m*-phenylene, the electronic impact of substituent will be centered near the middle or edge of the chromophore, respectively. Such arrangement in substitution is anticipated to affect the electron density distribution along the chromophore, which will have direct impact on the charge injection process in the polymer layer. Substitution can also affect the morphology of the polymer films, which will not only influence the PL process in the film state, but may also play a positive role in improving the contact between the polymer film and LED electrode. In addition, a substituent placed on an *m*-phenylene exerts its electronic effect simultaneously on both chromophores, as two adjacent chromophores in PmPVpPV share a common *m*-phenylene unit.

Due to inclusion of two adjacent *m*-phenylene units, the chromophore of **26** contains two alkoxy substitutes. In addition, the alkoxy group in **26** is located at an *ortho*-position to vinylene, thereby generating similar electronic impact as that in **20**. Under an ideal situation, quantitative information about the substitution effect at *p*- and *m*-phenylene can be obtained by comparison of **20** and **26** with the simplest PmPVpPV **28** ("Y" = "H"). Insolubility of **28**, however, hampers such a comparison. To evaluate the substitution impact at *m*- and *p*-phenylene on the optical properties of PmPVpPV materials, an alternative approach is to synthesize polymer **27**, in which the substituents are present on both *m*- and *p*-phenylenes. Comparison between the optical properties of **20**, **26**, and **27** is expected to provide some useful information to reveal the impact of substitution pattern on PmPVpPV materials.

Polymer Synthesis. Polymerization of 2,5-bis(hexyloxy)benzene-1,4-dialdehyde with 2-hexyloxy-5-methyl-1,3-xylene tetraethyldiphosphonate in THF under the presence of potassium *tert*-butoxide produced yellow polymer **27** (Scheme 5). The obtained polymer **27** was readily soluble in common organic solvents such as toluene, chloroform, and THF, partially ascribing to the increased alkyl side chain population on PmPVpPV

backbone. As anticipated from the Wittig-Horner condensation,[41] majority of the vinylene bonds (~61%) in **27** were in *trans*-configuration, on the basis of ^{1}H NMR analysis results. Size exclusion chromatography (SEC) with light-scattering detector showed that polymer **27** had a molecular weight of 10,600. The number-average degree of polymerization was estimated to be n≈12. Uniform thin film could be easily cast from its solution. To aid the structural analysis of **27**, a model compound **32** was prepared similarly by condensation of 2-(diethylphosphonate)-1-hexyloxy-4-methyl-benzene **31** with 2,5-bis(hexyloxy)benzene-1,4-dialdehyde **30**.

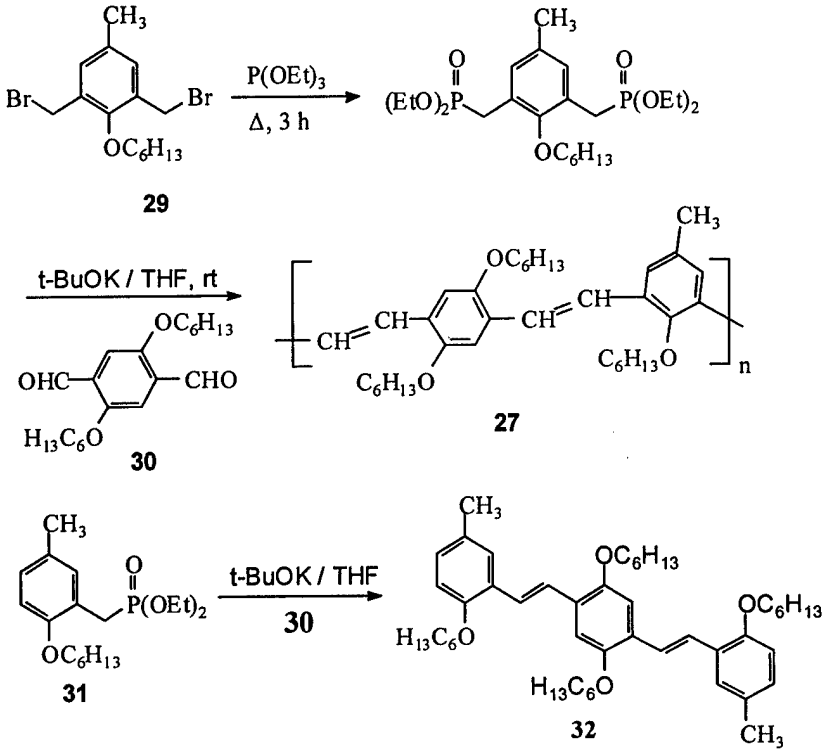

Scheme 5. Synthesis of polymer and its model compound.

Photoabsorption and Photoluminescence (PL). The UV-vis absorption and fluorescence spectra of **27** were acquired in dilute THF (Figure 21), in comparison with that of **20** and **26** under the same conditions. UV-vis absorption spectrum of **27** exhibited a major band (λ_{max} = 415 nm) and a minor band (λ_{max} = 332 nm), which was slightly red-shifted (~5 nm) from that of **20**. The observed bathochromic shift from **20** was due to the additional alkoxy and methyl groups on the *m*-phenylene of **27**. The absorption profile of **27** was very similar to that of **20**, but different from that of **26**, attributing to the common structural unit 2,5-alkoxy-1,4-phenylene present in both **20** and **27**. The spectral similarity between **20** and **27** also indicated that the electronic band structure of PmPVpPV might be more sensitive to perturbation from *p*-phenylene unit, which is located near the center of the chromophore.

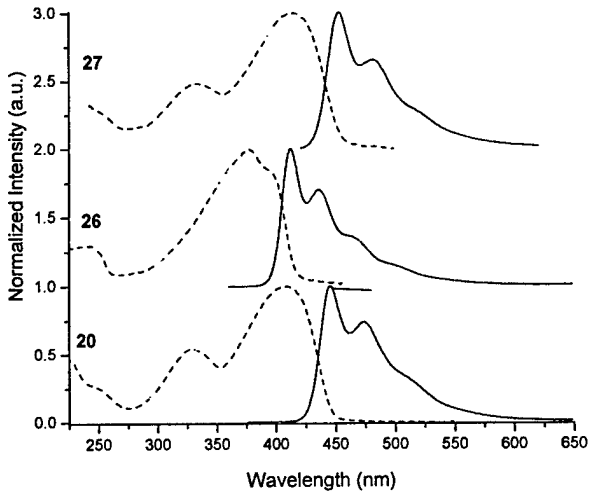

Figure 21. UV-vis (dotted line) and PL (solid line) of polymers **27** (top), **26** (middle), and **20** (bottom) in dilute THF solutions at room temperature.

It should be noted that there were three possible structural fragments (**33**, **34**, and **35**) randomly distributed along the polymer chain **27**, as a result from effective π-conjugation interruption at *m*-phenylene linkage. Since a *trans*-olefin permits a longer conjugation length than the corresponding *cis*-olefin,[42] the fragment **33** with both olefins

in *trans*-configuration will have a lower band-gap than the isomeric fragments **34** (with *cis*-, *trans*-configuration) and **35** (with *cis*-, *cis*-configuration). When these chromophores are jointed next to each other via sharing a common *m*-phenylene bridge, intramolecular energy transfer[43] would occur from a high band-gap chromophore (**34** or **35**) to a low band-gap chromophore (**33**), as observed from emission of PmPVpPV with different ratio of *cis*-/*trans*-CH=CH.[26] As a result, emission of polymer **27** is solely from the low band-gap **33**, and its emission spectrum will not be affected by different *cis*-/*trans*-CH=CH ratio present in the polymer structure. In contrast to its emission, the optical absorption of polymer **27** consisted of contribution from all chromophores **33-35**.

Fluorescence of polymers in THF revealed the similar trend as observed in absorption spectra, showing that the emission λ_{max} of **27** was slightly red-shifted from that of **20** (by ~8 nm). The emission profile of **27** was similar to that of **20** and **26**, with a major band at higher energy and a minor band at lower energy. As seen from Table 4, the high-energy emission band of **27** (λ_{max} =453 nm) was red-shifted by about 8 nm from that of **20** (λ_{max} = 445 nm), and by about 41 nm from that of **26** (λ_{max} = 412 nm). Larger bathochromic shift observed from **26** to **27** than that from **20** to **27** indicated that the alkoxy substitution on the *p*-phenylene was more effective in tuning the emission color of PmPVpPV, which was consistent with that observed in the absorption spectra. Fluorescence quantum efficiency of **27** in THF was estimated to be 0.78, which was higher than **20** (ϕ_{fl} = 60%) and **26** (ϕ_{fl} = 71%), further revealing the substitution impact to molecular luminescent properties of PmPVpPV. The observed higher fluorescence efficiency could be ascribed to the higher alkoxy population present on the chromophore of **27**, which is known to improve the fluorescence of an aromatic organic molecule.[44]

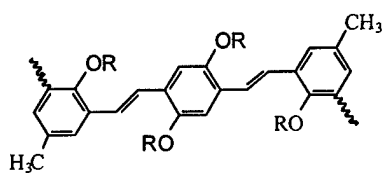

33

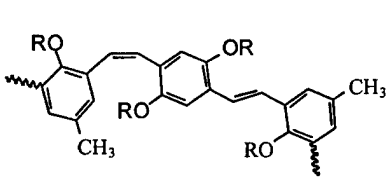

34

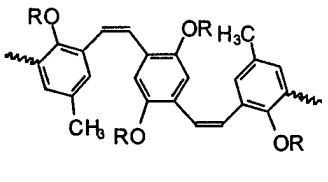

35

As pointed out in the earlier sections, the substituent located on the *m*-phenylene of PmPVpPV exerts its substitution effect simultaneously to two adjacent chromophores. A natural concern is whether the substitution effect on the *m*-phenylene is diluted. To address this question, spectral comparison was made between the model compounds **36**, **37**, and **32**, which closely represent the chromophores in polymers **20**, **26**, and **27**, respectively. The alkoxy and methyl substituents on the side phenyl rings of these model compounds are no longer shared between two chromophores. Comparison between these model compounds (Table 5 and Figure 22) showed that the high-energy emission band of **32** (λ_{max} =448 nm) was red-shifted by 9 nm from that of **36** (λ_{max} =439 nm), and by 36 nm from that of **37** (λ_{max} =412 nm). In other words, the magnitude of the substitution effect observed from the model compounds **32**, **37**, and **36** was similar to that observed from PmPVpPVs **27**, **26**, and **20**. The results strongly suggested that the substitution effect on the *m*-phenylene was not diluted, despite the fact that *m*-phenylene is shared between the two adjacent chromophores.

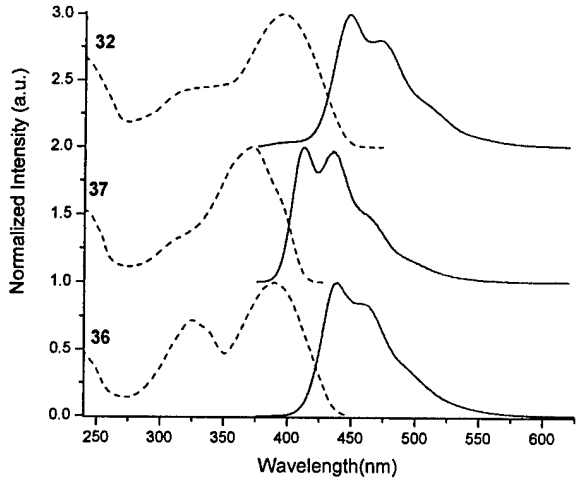

Figure 22. UV-vis (dotted line) and fluorescence (solid line) spectra of model compounds **36** (bottom), **37** (middle), and **32** (top)at ambient temperature.

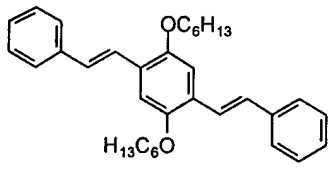

36

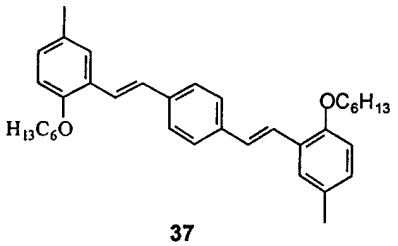

37

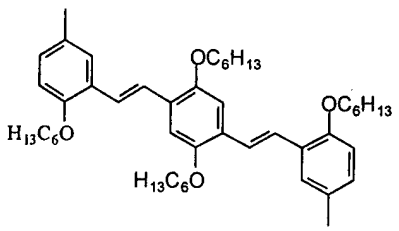

32

The absorption and fluorescence λ_{max} values of **32** were at 396 and 448 nm, respectively, which were quite comparable to that of polymer **27** at 415 and 453. The small difference in both absorption ($\Delta\lambda_{max}$ =9 nm) and emission ($\Delta\lambda_{max}$ = 5 nm) between the model chromophore **32** and polymer **27** was well within the anticipated substitution effect. In addition to their similar absorption and emission energy, nearly identical absorption and emission profiles between **32** and **27** further confirmed the presence of confined chromophore structure as a result of effective π-conjugation interruption at *m*-phenylene. Fluorescence quantum efficiency of **32** was estimated to be as high as 80%. Comparable fluorescence quantum efficiency between the polymers (**27**, **26**, and **20**) and their model compounds (**32**, **37**, and **36**) indicated that the high efficiency of the former was largely determined by its local chromophore structure.

Low Temperature UV-Vis and PL. The solution UV-vis spectrum of **27** at 25 °C showed peaks with λ_{max} at 332 and 415 nm (Figure 23). As temperature was lowered to −108 °C, the λ_{max} values were red-shifted to 337 and 434 nm, respectively, partially attributing to more *co*-planar conformation achieved at the low temperature. The fluorescence spectrum of **27** at −108 °C became more resolved than that at 25 °C. The emission bands were slightly red-shifted by about 5-7 nm to 458 and 489 nm (corresponding to the wavenumber of 21 834 and 20 450 cm^{-1}, respectively). The vibrational energy level of **27** in the ground state (as shown from its emission spectrum), therefore, was estimated to be about 1384 cm^{-1}, which is comparable with 1362 cm^{-1} for **26**[40] but notably smaller than 1659 cm^{-1} for **20**.[39] The vibrational energy gap of PmPVpPV appeared to be irregularly dependent on the substitution pattern on the polymer backbone, as the lone pair electron on alkoxy group can exert direct impact to the π-conjugated orbitals. The energy difference between overlapping low-energy absorption band (λ_{max} = 434 nm, or 23 041 cm^{-1}) and the high-energy emission band (λ_{max} = 458 nm, or 21 834 cm^{-1}) was estimated to be 1207 cm^{-1}, which is smaller than the required adjacent vibrational energy gap of at least 1384 cm^{-1} for a lower energy level in an oscillator model.[34] Therefore, it is likely that the emission band at about 458 and 489 nm are corresponding to 0–0 and 0–1 transitions, respectively. Further cooling the

solution to liquid nitrogen temperature (–198 °C) froze the solution to nontransparent solid, but did not clearly resolve the 0–2 band at about 525 nm.

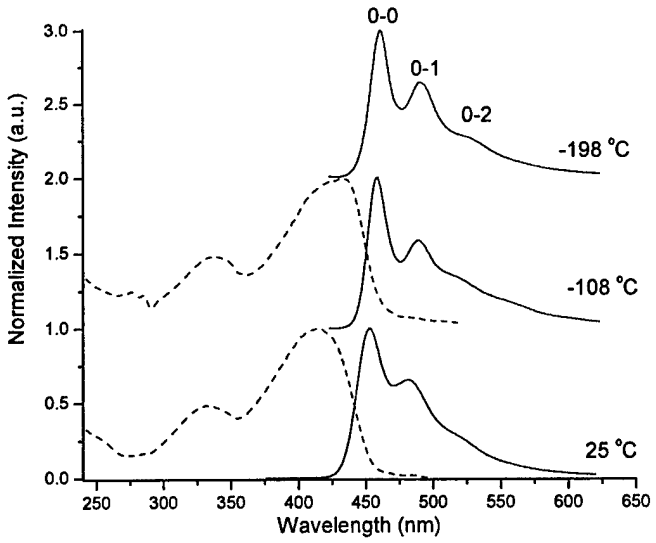

Figure 23. UV-vis and PL spectra of polymer **27** in THF solution at +25 °C, –108 °C, and –198 °C.

Optical Properties of Films. Polymers films **27**, **26**, and **20** were spin-cast on quartz plates from their respective THF solutions. Their UV-vis absorption and PL spectra were recorded at room temperature (Figure 24). The absorption profiles in the film states are very similar to that in their respective solutions, in agreement with the localized chromophore structures. The absorption peaks of polymer films are red-shifted from that of respective solutions by about 1 nm for **27**, 7 nm for **26**, and 21 nm for **20** (Table 4). In addition, the PL spectra of polymer films exhibits less structured feature in comparison with that of their respective solution spectra. Emission profile of **27** is characterized by a peak at 529 and a shoulder at about 557 nm, which is notably different from that of **26** (two peaks at 489 and 519 nm) and **20** (a shoulder at about 513 and a

peak at 531 nm). It appears that the substitution pattern plays an important role in the vibronic structure of PmPVpPV's emission. Observation of clearly resolved emission bands from film **26**, but not from films **27** and **20**, can be ascribed to the intrinsic property of a defined chromophore structure, as the emission spectrum of model compound **37** is better resolved than that of **32** and **36**. It is also noted that the emission of films is significantly red-shifted by about 80 nm from that of their respective solutions, in sharp contrast to the small bathochromatic shift observed in the absorption spectra. The results suggest a stronger chromophore-chromophore interaction occurred in the excited state than that in the ground state, leading to possible fluorescence excimer formation.

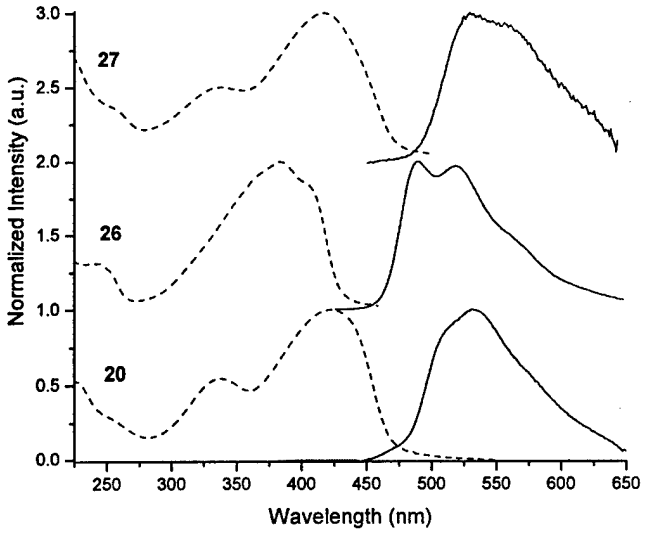

Figure 24. UV-vis (dotted line) and PL (solid line) of polymer films **27** (top), **26** (middle), and **20** (bottom) at room temperature.

EL properties of polymers were examined by fabricating double layer LEDs of configuration ITO/PEDOT/polymer/Ca. The EL spectrum of film **27** (Figure 25) exhibits a peak with $\lambda_{max} \approx 533$ nm, which closely matches the PL peak at 529 nm. Similarity between the PL and EL spectra of **27** suggests that both PL and EL originate from the same radiative decay process of the singlet exciton.[45,46] The EL peak of **27** is red-shifted from **20** (by ~10 nm)[39] and **26** (by ~37 nm),[40] in consistency with the trend observed in film PL spectra (Table 4). The current density and luminance vs voltage curves for LEDs are shown in Figure 26. Under the same device configuration, a balanced electron/hole injection is achieved in film **20**, since the turn-on voltages for current and light are the same. This desirable balance in charge injection is lost in films **26** and **27**, though at different degree, suggesting that charge injection property of PmPVpPV is sensitive to perturbation from substitution on *meta*-phenylene. The imbalanced electron/hole injection is clearly responsible for the relatively lower EL efficiency of **26** and **27** in comparison with that of **20** (Table 4). The device turn-on voltages are 9.5 V for **27**, 4.5 V for **26**, and 3.5 V for **20**, further showing the impact of *meta*-phenylene substitution to the performance of LEDs. The higher current turn-on voltage for **27** (~6 V) also indicates a higher charge injection barrier.

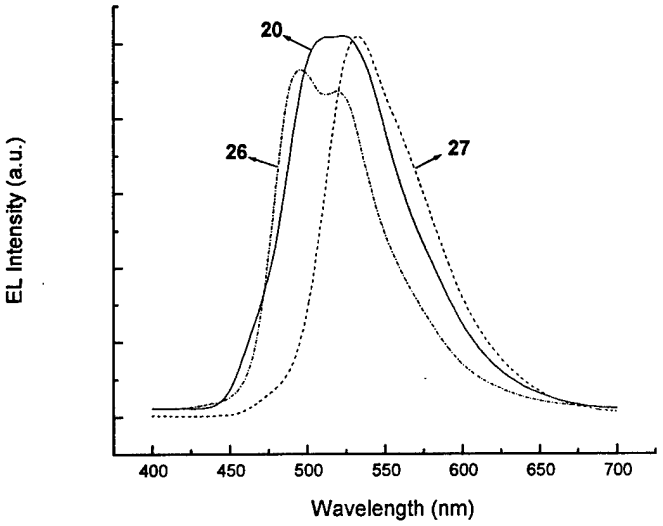

Figure 25. EL spectrum for device ITO/PEDOT/polymer **27**/Ca. EL spectra of **20** and **26** are shown for comparison.

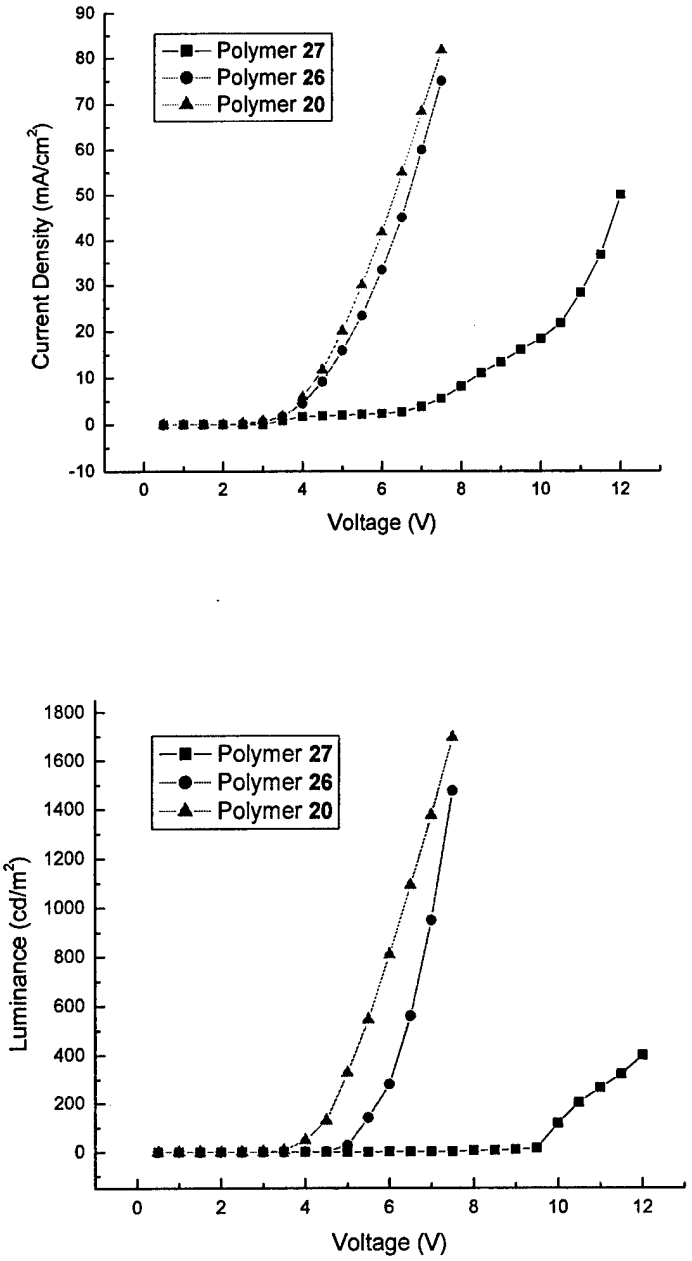

Figure 26. The voltage dependence of current density and luminance for device ITO/PEDOT/Polymer/Ca.

Table 4. Molecular weight, structure, and optical properties of polymers **27**, **26**, and **20**

Polymer	*trans*-CH=CH[a]	Mw/Mn(10^3)	Absorption λ_{max} (nm)[b]		Fluorescence λ_{max} (nm)[b]		ϕ_{fl}[c]	Φ_{EL}[d]
			solution	film	solution	film		
27	61%	10.6/6.27	332, **415**	337, **416**	**453**, 481	**529**, 557[sh]	78%	0.42%
26	84%	22/12.5	**377**, 396[sh]	**384**, 404[sh]	**412**, 436, 465	**489**, 519	71%	0.82%
20	96%	45/22.2	328, **410**	343, **431**	**445**, 474	513, **531**	60%[c]	0.91%

[a]The content of *trans*-CH=CH was estimated from ^{1}H NMR spectra in $CDCl_3$ solvent. [b]The spectra were acquired from solutions in THF or films cast from THF solution. The **bold** number indicates the most intense peak. [c]Fluorescence quantum efficiencies (ϕ_{fl}) were measured from polymer solution in THF. [d]EL efficiency of polymers was measured by using device configuration ITO/PEDOT/polymer/Ca. Recalibration of our measurement system showed that the previously reported EL efficiencies for **20**[39] and **26**[40] were significantly smaller than their true values.

Table 5. Optical absorption and emission of model compounds **32**, **36**, and **37** at ambient temperature.

compound	*trans*-CH=CH[a]	Absorption λ_{max} (nm)[b]	Fluorescence λ_{max} (nm)[b]	ϕ_{fl}[c]	FWHM(nm)
32	99%	323^{sh}, **396**	**448**, 472	80%	58
36	95%	324, **390**	**439**, 458	61%[c]	57
37	93%	371	**412**, 435	88%	60

[a]The content of *trans*-CH=CH was estimated from ^{1}H NMR spectra in $CDCl_3$ solvent. [b]The spectra were acquired from THF solution. The **bold** number indicates the most intense peak. [c]Fluorescence quantum efficiencies (ϕ_{fl}) were measured from THF solution.

Publications

During the period from December 1, 1999 to May 31, 2003, the following publications have been achieved.

- *Macromolecules*, **2001**, *34*, 6756-6760 (L. Liao, Y. Pang, L. M. Ding and F. E. Karasz) "Synthesis, Characterization and Luminescence of Poly[(*m*-phenylenevinylene)-*alt*-(1,4-dibutoxy-2,5-phenylenevinylene)] with Different Contents of c*is*- and *trans*-Olefins."

- *Macromolecules*, **2001**, *34* (21), 7300-7305. (L. Liao, Y. Pang, L. Ding, F. E. Karasz) "Blue-Emitting Soluble Poly(*m*-phenylenevinylene) Derivatives."

- *Macromolecules*, **2001**, *34,* 9183-9188 (L. Ding, F. E. Karasz, Z. Lin, M. Zheng, L. Liao, Yi Pang). "Effect of Förster Energy Transfer and Hole Transport Layer on Performance of Polymer Light-Emitting Diodes."

- *J. Mater. Chem.*, **2001**, *11(12),* 3078-3081 (L. Liao, Y. Pang) "A Study on the Vibration Structure of Poly(phenylenevinylene)s via Low-Temperature UV-vis and Fluorescence Spectroscopy.".

- *Tetrahedron Lett.*, **2002**, *43(3),* 391-394 (J. Li, L. Liao, Y. Pang) "A Study of Vibronic Structures in the Optical Spectra of Oligo(thienylene ethynylene)s.".

- *Macromolecules*, **2002**, *35*, 3819-3824 (L. Liao, Y. Pang, L. Ding, F. E. Karasz) "Green-Emitting Poly[(2-alkoxy-5-methyl-1,3-phenylenevinylene)-*alt*-(1,4-phenylenevinylene)s: Effect of Substitution Patterns on the Optical Properties." .

- *Synthesis*, **2002**, 1261-1267 (Q. Chu, Y. Pang) "Synthesis and Optical Properties of Poly[(2-alkoxy-5-methyl-1,3-phenyleneethynylene)-*alt*-(1,3-phenyleneethynylene)s,".

- *Macromolecules* **2002**, *35,* 5720-5723 (L. Liao, Y. Pang, F. E. Karasz) "Comparison of Optical Properties between Blue-Emitting Poly(*m*-phenylene vinylene) and PPV Block-co-polymer.".

- *Macromolecules* **2002**, *35*, 6055-6059 (L. Liao, Y. Pang, L. Ding, F. E. Karasz) "Effect of Iodine-Catalyzed Isomerization on the Optical Properties of Poly[(1,3-phenylenevinylene)-*alt*-(2,5-dialkoxy-1,4-phenylene vinylene)]s.".

- *Macromolecules* **2002**, *35*, 7569-7574 (Q. Chu, Y. Pang, L. Ding, F. E. Karasz) "Synthesis, Chain Rigidity, and Luminescent Properties of Poly[(1,3-phenylene-ethynylene)-*alt*-tris(2,5-dialkoxy-1,4-phenyleneethynylene)]s".

- *Thin Solid Films*, **2002**, *417*, 147-150 (E. E. Gurel, Y. Pang, and F.E. Karasz) "Luminescence Properties of Modified Poly(m-phenylenevinylene)-alt-(p-phenylenevinylene): Effects of Side-Chain Length, Blending and Device" .

- *Macromolecules,* **2003**, *36,* 3848-3853 (Q. Chu, Y. Pang, L. Ding, F. E. Karasz) "Green-Emitting PPE-PPV Hybrid Polymers: Efficient Energy Transfer across *meta*-Phenylene Bridge." .

- *Synthetic Metals*, **2003** in press (J. Li, Y. Pang), "Synthesis and optical properties of poly[(*p*-phenyleneethynylene)-*alt*-(*m*-phenyleneethynylene)]s: Evidence of Intramolecular Energy Transfer across *m*-Phenylene." (Published online 1 April 2003)

- *Macromolecules,* **2003**, *36*, 4614-4618 (Q. Chu, Y. Pang) "Molecular Aggregation of Poly[(1,3-phenyleethynylene)-*alt*-oligo(2,5-dialkoxy-1, 4-phenyleneethynylene)]: Effect of Solvent, Temperature, and Polymer Conformation." .

- *J. Polym. Sci. Part A: Polym. Chem.*, **2003**, *41,* 2650-2658 (L. Liao, Y. Pang, L. Ding, F. E. Karasz) "Blue-Emitting Poly[(*m*-phenylene vinylene)-*alt*-(*o*-phenylene vinylene)]s: Effect of Regioregularity on the Optical Properties." .

- *J. Polym. Sci. Part A: Polym. Chem.* **2003**, *41*, 3149-3158 (L. Liao, Y. Pang, L. Ding, F. E. Karasz) "A Yellow Light-Emitting Cyano-Substituted Poly[(1,3-phenylenevinylene)-*alt*-(1,4-phenylenevinylene)] Derivative: Its Synthesis and Optical Properties".

- *Macromolecules*, **2003**, *36*, 7301-7307 (L. Ding, F. E. Karasz, Y. Lin, L. Liao, Y. Pang) "Photoluminescence and Electroluminescence Study of Violet-Blue and Green-Emitting Polymers and Their Blend."

- Q. Chu, Y. Pang "Vibronic Structures in the Electronic Spectra of Oligo(phenylene ethynylene): Effect of *m*-Phenylene to the Optical Properties of Poly(*m*-phenylene ethynylene)" *Spectrachimica Acta Part A: Molecular and Biomolecular Spectroscopy,* in press.

- L. Liao, L. Ding, F. E. Karasz, Y. Pang, "Poly[(2-alkoxy-5-methyl-1,3-phenylene vinylene)-*alt*-(phenylene vinylene)] Derivatives with Different Content of *cis*-and *trans*-Olefins: Effect of Olefin Bond Geometry and Conjugation Length to Luminescence." *J. Polym. Sci. Part A: Polym. Chem.* accepted for publication.

Conclusion

During the reporting period, we have systematically examined the role of a *meta*-phenylene in the π-conjugated polymers. Resulting form its effective π-conjugation interruption, controllable insertion of *m*-phenylene along the polymer backbone is demonstrated to be a useful tool for precise color tuning. Introduction of a bent angle at the *m*-phenylene unit also improves the molecular packing in the solid state, thereby enhancing the PL quantum efficiency in the solid state. Although original investigation is focusing on the poly(phenylene ethynylene) system, the concept has been successfully extended to poly(phenylene vinylene) system.

By synthesis of polymers with defined chemical structures, we have investigated the impact of trace iodine to the luminescent properties of polymers. The results show that the Wittig-Horner reaction is a preferred method to construct the vinylene bond of *trans*-configuration. It is noted that there are two types of phenyl rings, i.e., *m*- and *p*-phenyl rings, present along the PPV chain examined. Selective placement of substituent on the different type of phenyl rings is found to significantly affect the luminescent properties of the polymers. Through collaboration with Professor Karasz's group at UMass, many of the polymers are shown be electroluminescent with EL efficiency reaching as high as ~1%. The EL efficiency of this class of materials will be further increased by improving the charge injection within the polymer layer.

Reference List

(1) Kraft, A.; Grimsdale, A. C.; Holmes, A. B. *Angew.Chem.Int.Ed.* **1998**, *37*, 402-428.

(2) McQuade, D. T.; Pullen, A. E.; Swager, T. M. *Chem.Rev.* **2000**, *100*, 2537-2574.

(3) McGehee, M. D.; Heeger, A. J. *Advanced Materials* **2000**, *12*, 1655-1668.

(4) Burroughes, J. H.; Bradley, D. D. C.; Brown, A. R.; Marks, R. N.; MacKay, K.; Friend, R. H.; Burn, P. L.; Holmes, A. B. *Nature* **1990**, *347*, 539-541.

(5) Bunz, U. H. F. *Chem.Rev.* **2000**, *100*, 1605-1644.

(6) Pang, Y.; Li, J.; Hu, B.; Karasz, F. E. *Macromolecules* **1998**, *31*, 6730-6732.

(7) Trumbo, D. L.; Marvel, C. S. *J.Polym.Sci.: Part A: Polym.Chem.* **1986**, *24*, 2311-2326.

(8) Moroni, M.; Moigne, J. L. *Macromolecules* **1994**, *27*, 562-571.

(9) Cotts, P. M.; Swager, T. M.; Zhou, Q. *Macromolecules* **1996**, *29*, 7323-7328.

(10) Chu, Q.; Pang, Y.; Ding, L.; Karasz, F. E. *Macromolecules* **2002**, *35*, 7569-7574.

(11) Chu, Q.; Pang, Y. *Synthesis* **2002**, 1261-1267.

(12) Swanson, L. S.; Shinar, J.; Ding, Y. W.; Barton, T. J. *Synthetic Metals* **1993**, *55-57*, 1-6.

(13) Swanson, L. S., Lu, F., Shinar, J., Ding, Y. W., and Barton, T. J. Poly(p-phenylene acetylene) (PPA)-Based Light-Emitting Diodes. Conwell, E. M., Stolka, M., and Miller, M. R. 1910, 101-110. 1993. SPIE Conf. Proc.

(14) Montali, A.; Smith, P.; Weder, C. *Synthetic Metals* **1998**, *97*, 123-126.

(15) Pschirer, N. G.; Miteva, T.; Evans, U.; Roberts, R. S.; Marshall, A. R.; Neher, D.; Myrick, M. L.; Bunz, U. H. F. *Chem.Mater.* **2001**, *13*, 2691-2696.

(16) Fiesel, R.; Halkyard, C. E.; Rampey, M. E.; Kloppenburg, L.; Studer-Martinez, S. L.; Scherf, U.; Bunz, U. H. F. *Macromol.Rapid Commun.* **1999**, *20*, 107-111.

(17) Jakubiak, R.; Collison, C. J.; Wan, W. C.; Rothberg, L. J.; Hsieh, B. R. *J.Phys.Chem.* **1999**, *A103*, 3294-3298.

(18) Schouwink, P.; Schäfer, A. H.; Fuchs, H. *Thin Solid Films* **2000**, *372*, 163-168.

(19) Chu, Q.; Pang, Y. *Macromolecules* **2003**, *36*, 4614-4618.

(20) J. D. Ingle, S. R. Crouch, Spectrochemical Analysis; Prentice Hall: Englewood Cliffs, 1988; pp344-347.

(21) J. Tsuiji, Palladium Reagents and Catalysts: Innovations in Organic Synthesis; Wiley: New York, 1996; pp168-178.

(22) The effect of a cyano substituent on benzene can lead to about 20 nm bathochromic shift on the primary pi-pi absorption band.[23]

(23) R. M. Silverstein, G. C. Bassler, T. C. Morrill; Spectrometric Identification of Organic Compounds, 5th ed.; John Wiley & Sons: New York, 1991; pp309-311.

(24) Demas, J. N.; Crosby, G. A. *J.Phys.Chem.* **1971**, *76*, 991-1024.

(25) G. G. Guilbault; Practical Fluorescence, 2nd ed.; Marcel Dekker: New York, 1990; pp146-154.

(26) Pang, Y.; Li, J.; Hu, B.; Karasz, F. E. *Macromolecules* **1999**, *32*, 3946-3950.

(27) Guilbault, G. G. Practical Fluorescence, 2nd ed.; Marcel Dekker: New York, 1990; Chapter 3.

(28) Ideses, R.; Shani, A. J. Am. Oil Chem. Soc. **1989**, *66*(7), 948-952.

(29) Liao, L.; Pang, Y.; Ding, L.; Karasz, F. E. *Macromolecules* **2001**, *34*, 6756-6760.

(30) Huang, C.; Huang, W.; Guo, J.; Yang, C.-Z.; Kang, E.-T. *Polymer* **2001**, *42*, 3929-3938.

(31) Star, A.; Stoddart, J. F.; Steuerman, D.; Diehl, M.; Boukai, A.; Wong, E. W.; Yang, X.; Chung, S.-W.; Choi, H.; Heath, J. R. *Angew.Chem.Int.Ed.Engl.* **2001**, *40*, 1721-1725.

(32) Ideses, R.; Shani, A. J. Am. Oil Chem. Soc. 1989, 66(7), 948-952.

(33) The repeating unit of **18a** has a formula $C_{28}H_{36}O_2$ (Mw = 404.6), which contains two phenylenevinylene units. The average molar mass of 202.3 for phenylenevinylene in **18a** is, therefore, used in the calculation.

(34) Turro, N. J. *Modern Molecular Photochemistry*; University Science: Mill Valley, CA, 1991.

(35) Sheridan, A. K.; Lupton, J. M.; Samuel, I. D. W.; Bradley, D. D. C. Synth. Met. 2000, 111-112, 531-534.

(36) Davey, A. P.; Maier, S.; Byrne, H. J.; Blau, W. J. *Synth.Met.* **1999**, *103*, 2478-2479.

(37) Ohnishi, T.; Doi, S.; Tsuchida, Y.; Noguchi, T. American Chemical Society: Washinton,DC, 1997; pp 345-357.

(38) Liao, L.; Pang, Y.; Ding, L.; Karasz, F. E. *Macromolecules* **2001**, *34*, 6756-6760.

(39) Liao, L.; Pang, Y.; Ding, L.; Karasz, F. E. *Macromolecules* **2002**, *35*, 6055-6059.

(40) Liao, L.; Pang, Y.; Ding, L.; Karasz, F. E. *Macromolecules* **2002**, *35*, 3819-3824.

(41) Wadsworth, W. S. *Org.React.* **1977**, *25*, 73.

(42) Lambert, J. B.; Shurvell, H. F.; Lightner, D. A.; Cooks, R. G. *Organic Structural Spectroscopy*; Prentice-Hall: Upper Saddle River, NJ, 1998; p 289.

(43) Efficient energy transfer through an m-phenylene bridge has been observed from m-phenylene-containing poly(phenyleneethynylene) system. J. Li, Y. Pang, Synthetic Metals, in press.

(44) Ingle, J. D.; Crouch, S. R. *Spectrochemical Analysis*; Prentice-Hall: Englewood Cliffs, New Jersey, 1988; pp 344-347.

(45) Baigent, D. R.; Friend, R. H.; Lee, J. K.; Schrock, R. R. *Synthetic Metals* **1995**, *71*, 2171-2172.

(46) Zhan, X.; Liu, Y.; Wu, X.; Wang, S.; Zhu, D. *Macromolecules* **2002**, *35*, 2529-2537.